

UNIVERSITI  
TEKNOLOGI  
PETRONAS

## **Correlation between Wax Content and Wax Texture**

by

Ahmad Hisham Bin Zakariah

10601

Dissertation submitted in partial fulfillment of

the requirements for

Bachelor of Engineering (Hons)

(Chemical Engineering)

SEPTEMBER 2011

University Teknologi PETRONAS  
Bandar Seri Iskandar  
31750 Tronoh  
Perak Darul Ridzuan

**CERTIFICATION OF APPROVAL**

**Correlation between Wax Texture and Wax Content**

by

**Ahmad Hisham Bin Zakariah**

A project dissertation submitted to the  
Chemical Engineering Programme  
University Teknologi PETRONAS  
in partial fulfillment of the requirement for  
BACHELOR OF ENGINEERING (Hons)  
(CHEMICAL ENGINEERING)

Approved by,

.....  
(Dr. Lukman Ismail)

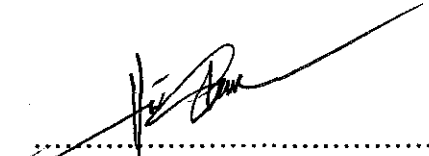
**UNIVERSITI TEKNOLOGI PETRONAS**

**TRONOH, PERAK**

**SEPTEMBER 2011**

## CERTIFICATION OF ORIGINALITY

This is to certify that I am responsible for the work submitted in this project, that the original work is my own except as specified in the references and acknowledgement, and that the original work contained herein have not been undertaken or done by unspecified sources or persons.



.....  
(Ahmad Hisham Bin Zakariah)

## **Acknowledgement**

During the completion of this project from the Final Year Project I till Final Year Project II, assistance, guidance and support had been given by many parties. From the starting point of topic selection, thorough research on literature review, work execution until the final stage that yield results, the project supervisor, Dr. Lukman Ismail had continuously encourage and provide guidance and support. The author would like to express the utmost gratitude to project supervisor, Dr. Lukman Ismail in spending his precious time despite his busy schedule and routine to monitor the project progression both as supervisor and coordinator.

Apart the project supervisor, the author would also like to express his appreciation to the lab technologist Mr. Mohd Fazli Zainal in his willingness to share his knowledge with the author and tending every needs of the author without fail. This had been helpful to the author towards the completion of this project. The authors also wish to acknowledge the materials, equipment and financial support provided by Department of Chemical Engineering, UTP and Universiti Teknologi PETRONAS. The author would like to extend the gratitude to technicians and colleagues who had helped, advised, guided and shared knowledge throughout this final year project period. A grateful appreciate is addressed to all who had contributed to the accomplishment of this project, for the constant encouragement and timely help throughout.

## **Abstract**

The gelling of waxy crudes and the deposition of wax on the inner walls of subsea crude oil pipelines present a costly problem in the production and transportation of oil. The objective of this work is to investigate the correlation between wax content and wax texture by understanding the mechanism and kinetics of the wax crystallization in accordance to Avrami theory. Another is to understand the texture of wax by using Leatherhead Food Research Association Texture Analyzer. The scopes of study for this project involve investigating of the effect of parameters such as temperature, wax composition and organic solvent variance. There will be two different types of solvents and these two will be mixed at three different weight percentages to assume several different oil models which will be tested on two sets of experimentation that is LFRA at three different point of temperature. For LFRA Texture analysis, a generalized texture profile analysis curve is expected to be obtained such as in Instron Universal Testing Machine. From the curve, several texture profile parameter can be identified and a correlation will be made. It is found that hardness plays a significant role in wax texture and wax content. An absolute correlation can be made from the three scopes of study.

## Table of Contents

CHAPTER 1: INTRODUCTION .....	8
1.1 Project Background.....	8
1.2 Problem Statement.....	9
1.3 Aim and objectives .....	9
1.4 Scope of Study .....	10
CHAPTER 2: LITERATURE REVIEW .....	11
CHAPTER 3: METHODOLOGY/PROJECT WORK .....	26
3.1 Research Methodology .....	26
3.2 Gantt Chart & Key Milestone.....	27
3.2 Work Breakdown Mapping.....	28
3.3 Project Activity .....	29
3.3.1 Wax Characterization.....	29
3.3.2 Sample Preparation .....	31
3.3.3 Experimentation.....	32
3.4 Tools Required.....	33
3.4.1 Equipment.....	34
3.4.2 Chemicals.....	34
3.4.3 Apparatus .....	34
CHAPTER 4: RESULTS AND DISCUSSIONS.....	35
4.1 Wax Characterization .....	35
4.2 LFRA Texture Analysis.....	35
4.2.1 Effect of Solvent.....	37
4.2.2 Effect of Temperature.....	39
4.2.3 Effect of Composition.....	41
CHAPTER 5: CONCLUSION AND RECOMMENDATION.....	44
REFERENCES .....	i
APPENDIX.....	v

## List of Tables

Table 2.1: Dimensional Analysis of TPA Parameters (Bourne, 1966a).....	23
Table 2.2: Parameter and definitions for Texture Profile Analysis .....	25
Table 3.1: FYP II Milestone .....	27
Table 3.2: Wax properties.....	30
Table 3.3: Wax-Diesel oil modeling with different wax composition.....	32
Table 3.4: Wax-Octane oil modeling with different wax composition.....	32
Table 3.5: Wax-Hexane oil modeling with different wax composition.....	32
Table 3.6: LFRA Standard Settings .....	33
Table 4.1: Results of Wax Characterization .....	35

## List of Figures

Figure 2.1: Variation of melting point (MP), transition temperature (TrT), and boiling point (BP) of normal alkanes with their number of carbon atoms (Himran & Suwono, 1994).....	12
Figure 2.2: Variation of the melting point and density (at 20°C) of normal alkanes with the number carbon atoms in alkanes (Himran & Suwono, 1994).....	12
Figure 2.3: LFRA Texture Analyzer.....	13
Figure 2.4: Schematic representation of the five different types of force-distance curves that are obtained in puncture tests. (Bourne,1979b).....	15
Figure 2.5: Schematic diagram of a simple cell for back-extrusion tests. (a) The plunger goes down and begins to contact the surface of the food; (b) The food is packed down and some liquid may be squeezed out; (c) The food is extruded through the annulus.....	16
Figure 2.6: Typical force-distance curve obtained with a simple compression-extrusion test. (de Man, Voisey, Rasper, and Stanley, eds.).....	18
Figure 2.7: Schematic diagram of the two compressions required for the texture profile analysis test. (a) Downstroke actions using the first and second bites; (b) upstroke actions during the first and second bites. (Bourne, 2002).....	20
Figure 2.8: A typical GF Texturometer curve (Bourne, 2002).....	21
Figure 2.9: A generalized texture profile analysis curve obtained from the Instron Universal Testing Machine (Bourne, 2002).....	22
Figure 2.10: Texture Profile Analysis test from Brookfield texture analyzer.....	24
Figure 3.1: Grinded wax.....	29
Figure 3.2: Moderate amount of grinded wax being heated.....	30
Figure 4.1: Wax-Hexane 30wt% solution at -4°C.....	36
Figure 4.2: Effect of Solvent toward Hardness.....	37
Figure 4.3: Effect of Solvent toward Adhesive Force.....	38
Figure 4.4: Effect of Solvent toward Adhesiveness.....	38
Figure 4.5: Effect of Solvent toward Resilience.....	39
Figure 4.6: Effect of Temperature toward Hardness.....	39
Figure 4.7: Effect of Temperature toward Adhesive Force.....	40
Figure 4.8: Effect of Temperature toward Adhesiveness.....	40
Figure 4.9: Effect of Temperature toward Resilient.....	41
Figure 4.10: Effect of Composition toward Hardness.....	41
Figure 4.11: Effect of Composition toward Adhesive Force.....	42
Figure 4.12: Effect of Composition toward Adhesiveness.....	42
Figure 4.13: Effect of Composition toward Resilience.....	43



## **CHAPTER 1: INTRODUCTION**

### **1.1 Project Background**

The name "paraffin" stems from the Latin "parum" (barely) and "affinis," with the meaning "lacking affinity" (Merriam-Webster Incorporated, 2011). This is because paraffin is very unreactive, as are all alkane. Approximately 3000 B.C., paraffin wax has actually already been discovered which is crystallized from petroleum. Paraffinic waxes compromise a broad group of opaque, water repellent, essentially solid materials having varied chemical that was identified dates back to Carl Reichenbach in 1830.

With the ongoing trend in deep water developments, flow assurance has become a major technical and economic issue. Many crude oils and crude oil products contain substantial fractions of petroleum wax. Deposition of paraffin wax is one of the major problems facing in the petroleum with the main implication being wax blockage in oil and gas pipelines especially for offshore production (Ismail, Westacott, & Xiongwei, 2007). The avoidance or remediation of wax deposition is one key aspect of flow assurance, thus the ability to predict wax deposition exceptionally becoming great importance. The objective of this work is to understand and build correlations between waxes content with temperature against wax properties itself such as gel strength, drip point, elasticity, yield points, pliability and other properties that LFRA Texture Analyzer capable to produce. There will be three different types of solvents and these two will be mixed at three different weight percentages to assume several different oil models. Only then the samples are tested using LFRA Texture Analyzer for results and findings at different temperatures up to minus four degree Celsius to promote the seabed-like temperature surroundings. These results will finally be discussed and analyzed with the LFRA experimentation to produce a correlation between them. An absolute correlation can be made from the three scopes of study. A straight correlation from temperature and solvents but a curve from solvents.

## **1.2 Problem Statement**

Although there are a lot of researches done on the wax analysis since last few decades but unfortunately there just research on a specific parameter of wax individually. There are not much data and research done on the correlation of wax texture and wax content. This knowledge will help to enhance the understanding on governing wax deposition in pipelines walls and removing accumulated wax in the most efficient and cost-effective means.

Mixing of paraffin with inorganic solvent always been a difficulty in room temperature. It is imperative to melt the wax while mixing the inorganic solvent and since the organic solvent boiling point usually at a low temperature, it would be far more difficult to mix paraffin wax in liquid form with organic solvent in gaseous form. Therefore it is vital to monitor the temperature of the system at all cost while mixing the two components at a certain most suitable temperature to ensure total system homogenous.

## **1.3 Aim and objectives**

This project aim is to study the correlation between characterizations of wax content with wax texture

While the subsequence objectives are:

1. To create several oil models using different composition and organic solvents
2. To conduct a texture analysis of oil model using LFRA (Leatherhead Food Research Association) Texture Analysis device

#### **1.4 Scope of Study**

The scope of study for this project is basically revolves in three variables that begin in oil modeling and throughout the experimentations. The variables are composition of wax, type of organic solvent and temperature of oil model during the testing. Sample preparation varied from 3 ranges of weight percent of wax in two or three different organic solvents. A laboratory work using texture analyzer hardness, adhesiveness, resilience, and adhesive force. Conducting relationship analysis between temperatures, organic solvents and compositions of wax texture and wax content by means of mathematical and deducing approach.

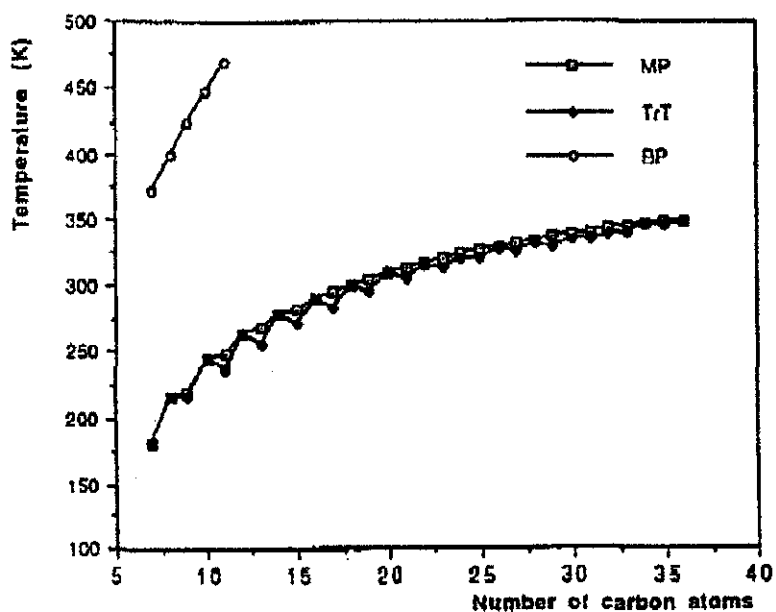
## CHAPTER 2: LITERATURE REVIEW

Paraffin wax is a composite material that is made up of a mixture of straight-chain hydrocarbon molecules. The molecular formula for paraffin is  $C_nH_{2n+2}$ , where the value of  $n$  ranges from 19 to 36 and the average value is 25 (Kirk-Othmer, 1999). It is originated from mineral oil or petroleum products consisting heavy hydrocarbons of alkanes. Presence of paraffin in crude oil could cause plugging problem due to wax buildup inside conduits such as well, pipeline, etc. during production, transportation and storage of petroleum crude (Kawanaka, Park, & Mansoori, 1991). It is found that paraffinic components contribute to the evolving gel strength (Kyeongseok, Mark, Pankaj, Jules, & Millind, 2006). This may prove that any solutions consist higher concentration of paraffin wax will have higher gel strength. It has been reported that the gel properties depend on various factors: temperature, cooling rate, cooling time, shear history and a diverse combination of factors (Kyeongseok, Mark, Pankaj, Jules, & Millind, 2006).

The behavior of waxy crudes usually approximated by modeling them as Bingham-like fluids. Different mathematical models have been proposed ranging from a general one-dimensional model of waxy crude to models that describe crude oils depositing wax in closed flow loops. For example, (Fusi, 2003) and (Fasano, Fusi, & Correr, 2004) delineate many models of differing complexity for the representation of waxy crude oils. In order to fully model the flow of these crude oils, the mechanisms governing the deposition and removal of solid wax must be incorporated into the model. Then the models can be developed, in formed by a theoretical understanding of the mechanisms at a play and the properties of the mixtures under study. However, the question arises of which mechanisms are actually relevant.

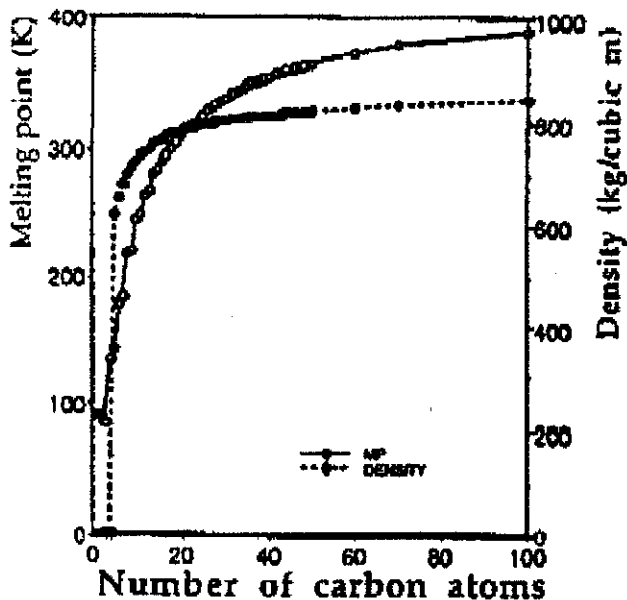
The lattice transition in alkanes is accompanied by the released of heat transition. Generally, lattice transition occurs in solid state at about 2 – 5 K below melting point. The difference between the transition temperature and melting temperature becomes smaller with increasing molecular weight and finally disappears for alkanes with more than 36 carbon (Mozes, 1982), as demonstrated in

Figure 2.1. The heat associated with this solid-solid transition is subtracted from the latent heat of melting.



**Figure 2.1: Variation of melting point (MP), transition temperature (TrT), and boiling point (BP) of normal alkanes with their number of carbon atoms (Himran & Suwono, 1994)**

Figure 2.2 show variations of melting point and density of normal alkanes versus increasing number of carbon atoms in their structures. According to this figure, the melting point and density versus the number of carbon atoms have a smooth variation (Himran & Suwono, 1994).



**Figure 2.2: Variation of the melting point and density (at 20°C) of normal alkanes with the number carbon atoms in alkanes (Himran & Suwono, 1994)**



**Figure 2.3: LFRA Texture Analyzer**

The LFRA (Leatherhead Food Research Association) is somewhat a type of UTM (Universal Testing Machine). The use of these instruments has become widespread during the last 20 years. UTMs consist of three essential components (Bourne et al., 1966), (Bourne, 2002).

A drive system that imparts motion to a cross-head that holds part of the test cell. The drive system may be double screw, single screw, hydraulic, chain or eccentric and lever system. High-force capacity Instron machines are driven by twin screws and low-force capacity models by a single screw. The standard TA.XT2 Texture Analyzer is driven by a single screw. The Food Technology Corporation Texture Test System is driven hydraulically, the General Foods Texturometer is driven by an eccentric and lever system and the Lloyd model TA5000 is driven by a chain.

Test cells that hold the food and apply force to it. The test cell comprises two parts. The lower part which is usually stationary is attached to the base of the

machine and supports or contains the food being tested. The upper part of the test cell is attached to the moving crosshead or arm. Different test cells can be installed that use any test principle requiring rectilinear movement including puncture, gentle compression for deformation, major compression for texture profile analysis, extrusion, cutting–shear, bending–snapping and tensile.

The puncture test measures the force required to push a punch or probe into a food. The test is characterized by

- (a) A force measuring instrument,
- (b) Penetration of the probe into the food causing irreversible crushing or flowing of the food
- (c) The depth of penetration is usually held constant.

When a punch is mounted in an instrument that automatically draws out a force–distance or force–time curve (such as the Instron or TA.XT2), five basic types of curves are obtained, as shown schematically in Figure 2.4. In types A, B, and C there is an initial rapid rise in force over a short distance of movement as the pressure tip moves onto the commodity. During this stage the commodity is deforming under the load; there is no puncturing of the tissues. This stage ends abruptly when the punch begins to penetrate into the food, which event is represented by the sudden change in slope called the *yield point*, or sometimes '*bio-yield point*.' The initial deformation stage is not of great concern in puncture testing.

The yield point marks the instant when the punch begins to penetrate into the food, causing irreversible crushing or flow of the underlying tissues and is the point of greatest interest in puncture testing. Mohsenin *et al.* (1963) showed that this is the point where crushing and bruising begins on fruits such as apples. Considerable work has been done on the implications of the yield point and this will be discussed below. The third phase of the puncture test, namely, the direction of the force change after the yield point and during penetration of the punch into the food, separates the puncture curves into three basic types: A, the force continues to increase after the yield point; B, the force is approximately constant after the yield point; C, the force decreases after the yield point. There is a continuous change in slope, from positive slope in type A curves to approximately zero slope in type B curves to negative slope

in type C curves. Type A curves merge into type B curves, depending on the steepness of the slope of the force– distance curve after the yield point, and, likewise, type B curves merge into type C curves. There are occasions when one needs to use subjective criteria to decide whether a curve is type A or B, or type B or C. The sensory and physical meaning of the difference between type A, B, and C curves is presently not well understood. Friction of the food along the sides of the punch accounts for a slightly increasing positive slope in a limited number of cases (for example, see Thompson *et al.*, 1992), but there are cases (e.g., freshly harvested apples) where friction cannot account for the increase in force after the yield point has been passed.

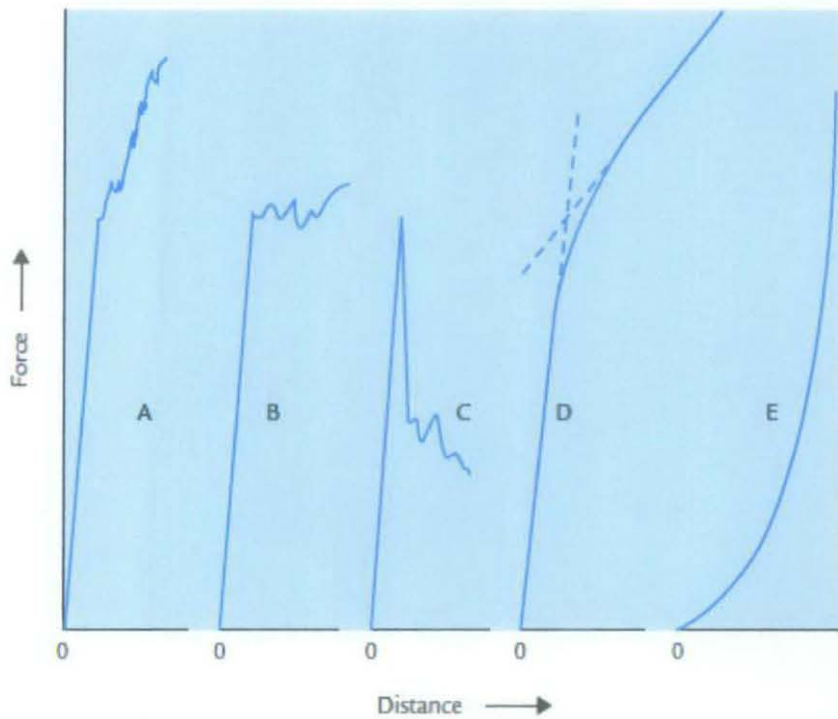


**Figure 2.4: Schematic representation of the five different types of force-distance curves that are obtained in puncture tests. (Bourne,1979b)**

A fourth type of curve, shown in curve D, is obtained on some starch pastes and whipped toppings and foams. It is essentially a type A curve except that the yield point is not sharply delineated by an abrupt change in slope; rather there is a gradual change in slope. The intersection formed by extrapolating the two straight-line portions of type D curves is usually a precise and reproducible point that can be used



as a yield point Figure 2.4; hence, a type D curve may be considered as a special case of a type A curve.

The type E curve is found with some starch pastes. This type of commodity shows no yield point, behaves essentially as a viscous liquid, and is unsuited to the puncture test because no meaningful results can be extracted from a type E puncture test curve at the present time.

The compression–extrusion test consists of applying force to a food until it flows through an outlet that may be in the form of one or more slots or holes that are in the test cell. The food is compressed until the structure of the food is disrupted and it extrudes through these outlets. Usually the maximum force required to accomplish extrusion is measured and used as an index of textural quality. This type of test is used on viscous liquids, gels, fats, and fresh and processed fruits and vegetables. Since extrusion requires that the food flow under pressure, it seems reasonable to use it on food that will flow fairly readily under an applied force and not to use it on those foods that do not flow easily, such as bread, cake, cookies, breakfast cereals, and candy.

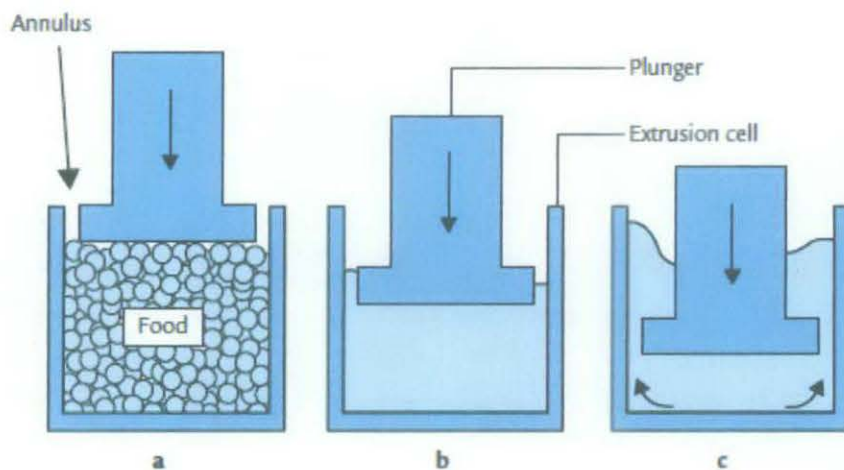


**Figure 2.5: Schematic diagram of a simple cell for back-extrusion tests. (a) The plunger goes down and begins to contact the surface of the food; (b) The food is packed down and some liquid may be squeezed out; (c) The food is extruded through the annulus**

A simple type of compression–extrusion test is shown in Figure 2.5, in which the food is placed in a strong metal box with an open top. A loose-fitting plunger is

then forced down into the box until the food flows up through the, space between the plunger and the walls of the box. This space is called the annulus.

In Figure 2.5a the food has been placed in a cell and the compressing platen has just contacted the surface. In Figure 2.5b the food, has been packed down solid so that the air between the particles has been removed. Figure 2.5c shows the actual process of extrusion where the food is forced to flow around the space between the edge of the compressing platen and the inside wall of the cell. This is called a 'back extrusion test' because the food moves in the opposite direction to the plunger.

The Ottawa Texture Measuring System (OTMS) (Voisey, 1971) uses a forward extrusion test because the food moves in the same direction as the plunger. Voisey and Nonnecke (1972b) developed test cells for the OTMS that are square in cross-section and 12.8 cm high. Four sizes of cells were made with cross-sectional areas of 20, 30, 40 and 50cm<sup>2</sup>. The 30cm<sup>2</sup> cell is the most widely used size. A separate frame holding either a series of parallel wires or a plate with a grid of holes in it fits into the bottom of the cell. A plunger that is square in cross-section and clears the inner walls by 0.75 mm is driven down into the cell forcing the food through the wires or holes and the force is measured.

Although the OTMS instrument is no longer commercially available, the OTMS test cells can be obtained from the Instron Corporation. The standard cell of the Food Technology Texture Press is mixed; half the food is extruded forward through the slits in the bottom of the cell and the other half is extruded backwards up between the descending blades.

A typical force-distance curve obtained from such an apparatus is shown in Figure 2.6. From A to B the food is deformed and compressed to pack more and more tightly into the diminishing space available under the descending plunger; there is almost no rupture or breaking of the food. At approximately the point B the food is packed solid and liquid begins to be pressed from high moisture foods such as fruits and vegetables filling the interstices. At point B or soon afterwards the pack is solid except for small amounts of entrapped air, and the force increases steeply from B to C pressing out more juice in the process. At point C the food begins to rupture and

flow up through the annulus, and this process continues to point D when the compressing platen reverses direction and the force falls to zero. Point C gives the force necessary to begin the process of extrusion, and the plateau CD shows the force needed to continue extrusion. From B to C represents the increasing force being applied to an almost incompressible mixture of solids and liquid.

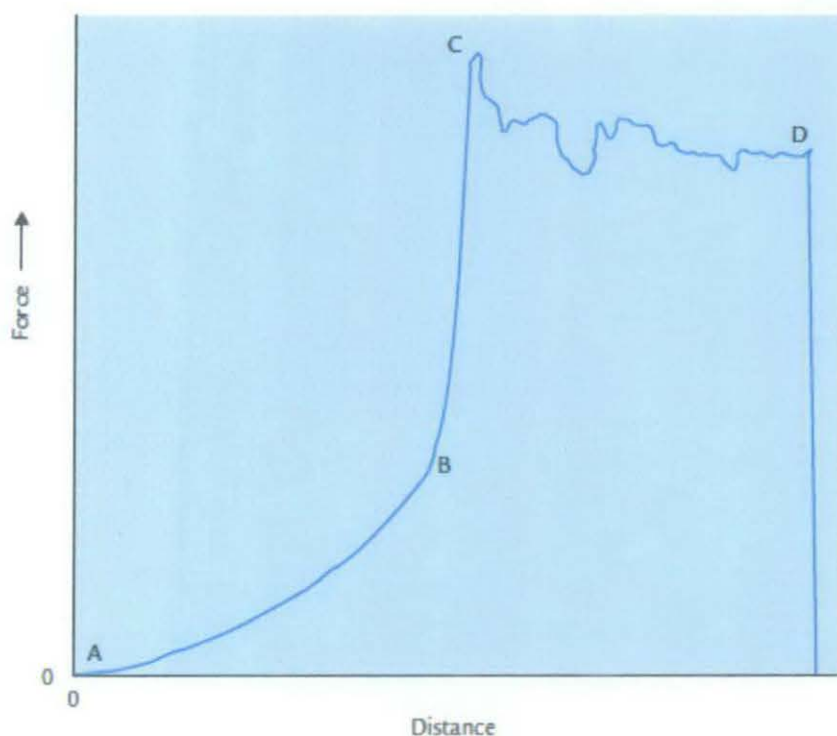


**Figure 2.6: Typical force-distance curve obtained with a simple compression-extrusion test. (de Man, Voisey, Rasper, and Stanley, eds.)**

The shape and magnitude of the compression–extrusion curve is influenced by the elasticity, viscoelasticity, viscosity, and rupture behavior of the material; sample size, deformation rate, sample temperature, type of test cell; sample test size; and homogeneity of the sample (Voisey *et al.*, 1972). With most processed fruits and vegetables and many other foods the plateau CD is horizontal or nearly so. The unevenness of the plateau is caused by variations in the firmness or toughness of the particles that are passing through the annulus zone at any particular time.

In general, the slope of the curve during the process of extrusion is approximately horizontal, but there are times when it will show a steadily increasing or decreasing

slope. According to Voisey *et al.* (1972), the slope of the extrusion part of the curve can indicate four different behavior patterns.

- (1) The force reduces rapidly with further compression. This indicates that the sample was compressed until a catastrophic failure occurred, indicating that resistance to shearing is the dominant mechanism of this test.
- (2) The force decreases slowly, indicating some shearing resistance combined with some extrusion and possibly adhesion of the sample to test cell.
- (3) An approximately horizontal plateau indicates either shearing of successive layers of the sample or a combination of shearing, extrusion, and adhesion occurring simultaneously.
- (4) The force steadily increases as extrusion proceeds. This indicates further compression of the sample in addition to various amounts of adhesion, extrusion, and shearing.

An advantage of UTMs is that the same basic machine can be configured for different kinds of tests. Previously, a new machine had to be purchased for every different kind of test. Another advantage is that the complete force history is plotted, giving all the changes that occur, including the rate of change (slopes), maximum force (peaks), fracture events (rapid decreases in force), area under the curve (work), and frequently other parameters of interest. The use of recorders tends to reduce confidence in the old one-point instruments that measure maximum force only. When a pointer moves over a dial and the maximum force reading is taken, there appears to be an element of certainty about the results that leads to a feeling of confidence in the instrument. When the same test is repeated in a recording instrument, the maximum force often seems to be an arbitrary point to use as an index of textural qualities; there is a loss of confidence in the accuracy of the test and the feeling of infallibility associated with some of these simple instruments is lost.

A group at the General Foods Corporation Technical Center pioneered the test that compresses a bite-size piece of food two times in a reciprocating motion that imitates the action of the jaw, and extracted from the resulting force–time curve a number of textural parameters that correlate well with sensory evaluation of those parameters (Friedman *et al.*, 1963; Szczesniak *et al.*, 1963). The instrument devised especially for this purpose is the General Foods Texturometer.

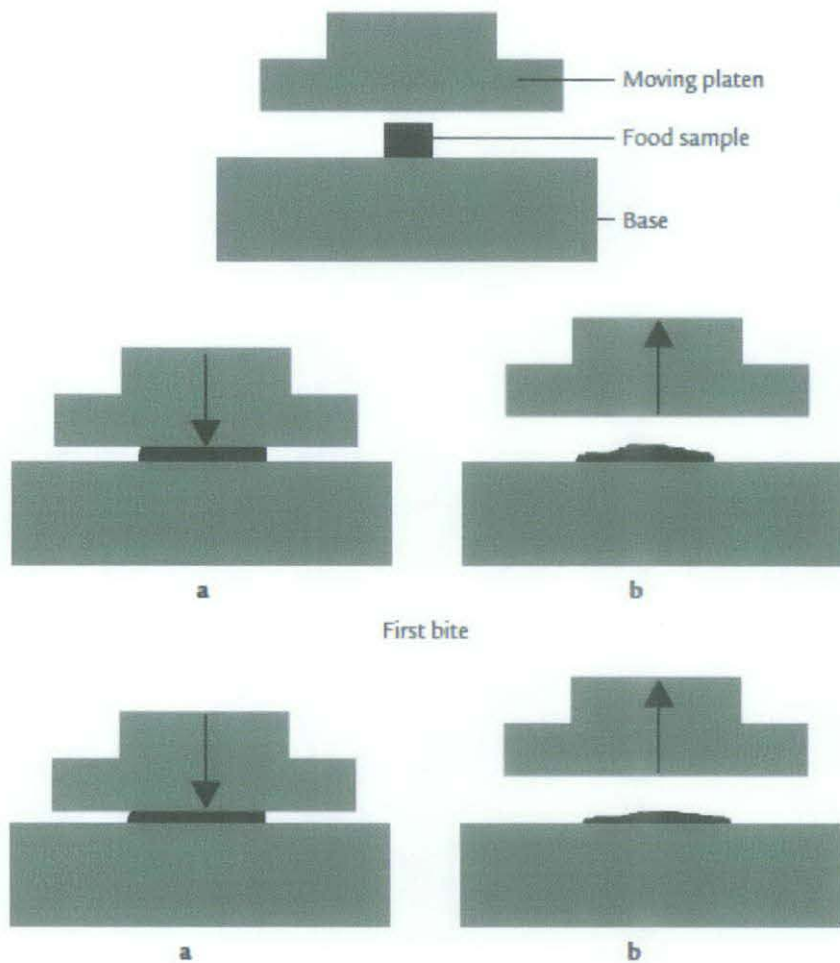


**Figure 2.7: Schematic diagram of the two compressions required for the texture profile analysis test. (a) Downstroke actions using the first and second bites; (b) upstroke actions during the first and second bites. (Bourne, 2002)**

The principle of the TPA test is illustrated in Figure 2.7: A ‘bite-size’ sample of food of standard size and shape is placed on the baseplate and compressed and decompressed two times by a platen attached to the drive system. To imitate the chewing action of the teeth there should be a high compression. The author usually uses a 90% compression when performing TPA tests in his laboratory. Figure 2.8 shows a typical TPA curve generated by the G. F. Texturometer. The height of the force peak on the first compression cycle (first bite) was defined as hardness; in Figure 2.8, A is the beginning of the first compression and B is the beginning of the second compression. Fracturability (originally called brittleness) was defined as the force of the significant break in the curve on the first bite (shown as a dashed line in Fig. 2.8). The ratio of the positive force areas under the first and second compressions ( $A_2/A_1$ ) was defined as cohesiveness. The negative force area of the

first bite ( $A_3$ ) represented the work necessary to pull the compressing plunger away from the sample and was defined as adhesiveness. The distance that the food recovered its height during the time that elapsed between the end of the first bite and the start of the second bite (BC) was defined as springiness (originally called elasticity). Two other parameters were derived by calculation from the measured parameters: gumminess was defined as the product of hardness  $\times$  cohesiveness; chewiness was defined as the product of gumminess  $\times$  springiness (which is hardness  $\times$  cohesiveness  $\times$  springiness). (Szczesniak & Hall, 1975) gave an updated account of the development and changes in the technique since 1963.

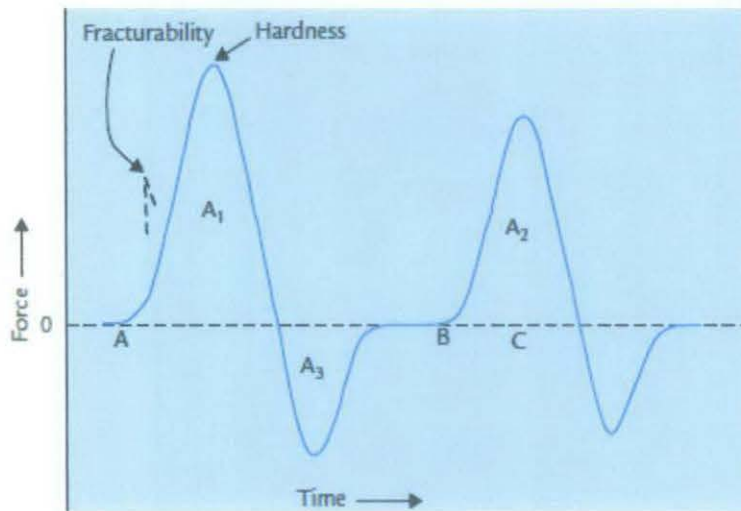


**Figure 2.8: A typical GF Texturometer curve (Bourne, 2002)**

In the original description of TPA chewiness was defined as the energy required masticating a solid food product and gumminess as the energy required to disintegrate a semisolid food to a state of readiness for swallowing. Szczesniak (1995) pointed out that the distinction has often been overlooked that gumminess and chewiness are mutually exclusive. Therefore, in reporting TPA measurements one should report either chewiness values, or gumminess values but not both for the same food.

The Instron, TA.XT2 Texture Analyzer and some other universal testing machines have been adapted to perform a modified texture profile analysis (Bourne, 1968, 1974). A typical Instron TPA curve is shown in Figure 2.9. Bourne closely followed the interpretation of Friedman et al. (1963) with one exception: instead of

measuring the total areas under the curves to obtain cohesiveness, he measured the areas under the compression portion only and excluded the areas under the decompression portions.

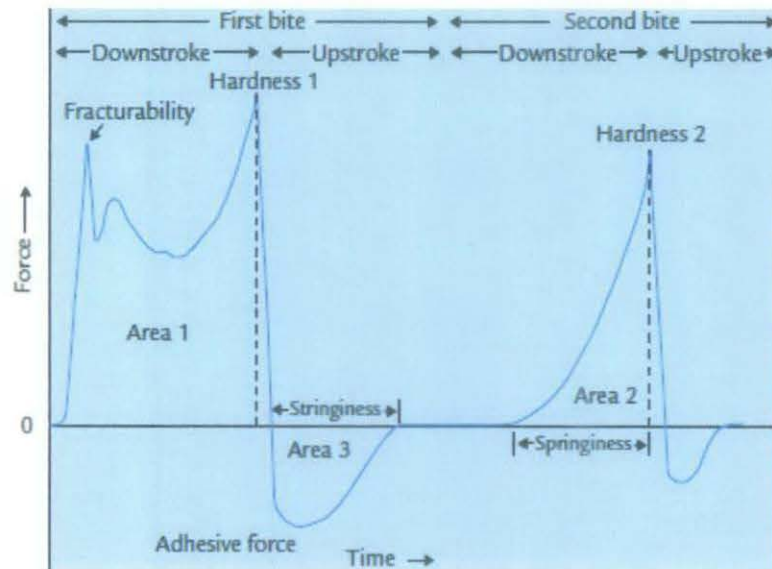


**Figure 2.9: A generalized texture profile analysis curve obtained from the Instron Universal Testing Machine (Bourne, 2002)**

A typical TPA curve obtained in the Instron differs in several major respects from that obtained by the GF Texturometer. This can be seen by comparing Figure 2.8 and 2.9. The Instron curves show sharp peaks at the end of each compression while the GF Texturometer shows rounded peaks. These differences arise from differences in instrument construction and operation. The GF Texturometer is driven by means of an eccentric rotating at constant speed and imparting a sinusoidal speed to the compressing mechanism, while the Instron is driven at constant speed. The GF Texturometer decelerates as it approaches the end of the compression stroke, momentarily stops, and then slowly accelerates again as it makes the upward stroke. In contrast, the Instron approaches the end of the compression stroke at constant speed, abruptly reverses direction and performs the upward stroke at constant speed. The constant speed of the Instron versus the continuously changing speed of the GF Texturometer largely accounts for the sharp peaks in the Instron in contrast to the rounded peaks of the Texturometer.

Another difference is that the supporting platform of the GF Texturometer is flexible; it bends a little as the load is applied. The Instron is so rigid that bending of the instrument can be ignored. Yet another difference is that the compressing plate of the Texturometer moves in the arc of a circle, whereas in the Instron it moves rectilinearly. These three factors taken together account for the differences in the TPA curves obtained by the GF Texturometer and the Instron.

**Table 2.1: Dimensional Analysis of TPA Parameters (Bourne, 1966a)**

<b>Mechanical Parameter</b>	<b>Measured variable</b>	<b>Dimensions of measured variable</b>
Hardness	Force	$mlt^{-2}$
Cohesiveness	Ratio	Dimensionless
Springiness	Distance	$l$
Adhesiveness	Work	$ml^2t^{-2}$
Fracture-ability (brittleness)	Force	$mlt^{-2}$
Chewiness	Work	$ml^2t^{-2}$
Gumminess	Force	$mlt^{-2}$

Since the Instron gives both a force–time and force–distance curve, the TPA parameters obtained from it can be given dimensions, which are listed in Table 2.2.

Henry et al. (1971) provided a more detailed analysis of the adhesiveness portion of texture profile curve for semisolid foods such as custard, puddings, and whipped toppings. In addition to measuring the area of the adhesiveness curve they measured its maximum force (symbolized by  $F_a$  to denote firmness under tension), the recovery in the adhesion portion between the first and second compressions ( $E_a$  to denote elastic recovery under tension), and the ratio of the two adhesion areas ( $C_a$  to denote cohesiveness under tension). They calculated gumminess under tension ( $Ch_a = F_a \times C_a \times E_a$ ). They also measured the property of stringiness (or, inversely, shortness) as the distance the product was extended during decompression before breaking off (Henry and Katz, 1969). Their experiments showed that eight of these parameters accounted for more than 90% of the variation of four sensory factors.

Reports on the Texture Profile Analysis of a number of commodities have appeared in the literature with some variations on the main themes described above. Breene (1975) gave a complete review of this area.



From a sample of Brookfield Texture analyzer show two graphs that show two ways of looking at the data from one 2 cycle Texture profile analysis test. The force vs. time graph clearly shows the force peak resulting from each compression cycle while the force vs. distance graph better displays the response of the sample to the application and removal of strain.

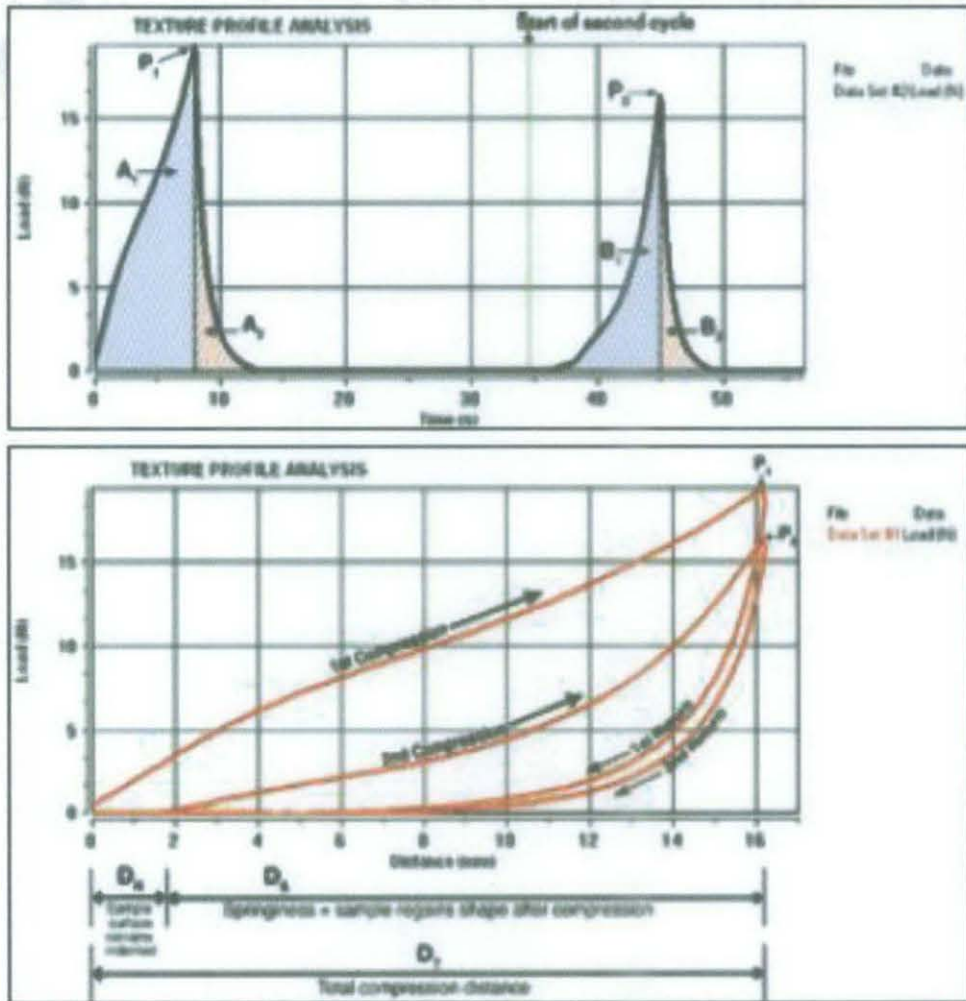


Figure 2.10: Texture Profile Analysis test from Brookfield texture analyzer

**Table 2.2: Parameter and definitions for Texture Profile Analysis**

<b>Parameter</b>	<b>Sensory Definition</b>	<b>Instrumental Definition</b>	
<b>Hardness</b>	Force required compressing a food between the molars. Defined as force necessary to attain a given deformation.	Peak force of the first compression cycle.	$P_1$
<b>Springiness Index</b> Preferred for comparing samples of different length	Ratio of the height the sample springs back after the first compression compared to the maximum deformation.	Springiness divided by total deformation.	$\frac{D_s}{D_T}$
<b>Corrected Cohesiveness</b> (Peleg, 1977)	Net work invested in the non-recoverable deformations of the first and second chews.	The ration of the net work of the second cycle $B_1 - B_2$ divided by that of the first cycle $A_1 - A_2$	$\frac{B_1 - B_2}{A_1 - A_2}$
<b>Corrected Chewiness</b>	The net energy required to chew a SOLID food to the point required for swallowing it.	The product of hardness, corrected cohesiveness and springiness index	$P_1 \times \frac{B_1 - B_2}{A_1 - A_2} \times \frac{D_s}{D_T}$
<b>Resilience</b> (Peleg, 1977)	Measurement of how a sample recovers from deformation in relation to speed and forces derived.	Resilience is the ratio of work returned by the sample as compressive strain is removed (known as recoverable work done $A_2$ ), to the work required for compression (known as hardness work done $A_1$ ).	$\frac{A_2}{A_1}$
<b>Adhesiveness</b>	The work necessary to overcome the attractive forces between the surface of the food and the surface of other materials with which the food comes into contact (e.g. tongue, teeth, palate). Work required to pull food away from a surface.	The negative area for the first bite, representing the work necessary to pull the compressing plunger away from the sample. (No adhesiveness is seen in graphs above.)	
<b>Adhesive Force</b> (Fizman & Damasio, 2000)	The maximum force required to separate teeth after biting sample.	Maximum negative force generated during probe return.	
<b>Gumminess</b> Applies to semi-solid products only if they have no springiness & undergo permanent deformation	Energy required to disintegrate a SEMI-SOLID food product to a state ready for swallowing. Related to foods with low hardness levels.	The product of hardness and cohesiveness	$P_1 \times \frac{B_1}{A_1}$
<b>Cohesiveness</b> A measurement of how well the structure	The strength of internal bonds making up the body of the product (greater the value the greater the cohesiveness)	The ratio of the work during compression (downward stroke only) of the second cycle $B_1$ divided by that of the first cycle $A_1$ .	$\frac{B_1}{A_1}$
<b>Chewiness</b> Solid foods only	The energy required to chew a SOLID food to the point required for swallowing it.	The product of hardness, cohesiveness and springiness.	$P_1 \times \frac{B_1}{A_1} \times D_s$

## **CHAPTER 3:     METHODODOLOGY/PROJECT WORK**

### **3.1   Research Methodology**

Before proceeding into work project, the desired findings have to be decided. In this case is to study mainly the characteristics of wax texture against different temperature and solvent. Each and every single step will be determine from here on out.

Another essential preliminary task is to review the literature to acquaint with the available body of knowledge in the area of interest. Literature review is the integral part of entire research process and makes valuable contribution to every operation step. Though it is time-consuming, intimidating and daunting, it brings great importance to enhance clarification and focus in the area of interest. It helps to improve methodology while broaden the knowledge in the area of interest and contextualize future findings. There are two main source of existing literature and they are books and journals. Books give advantage of good quality and integrated findings with other research to form coherent body of knowledge while journals will provide with the most up-to-date information discarding their gap of years in completion research and publication journals.

After identifying books, journals and articles, the next step is to reading them critically to pull together themes and issues that are associated. There three things to be concern with, one is to note whether the knowledge is relevant to the theoretical framework and it is confirmed beyond doubt. Two is to note the theories that are highlighted, their basis and methodologies adaptation. Three is to examine whether the findings can be generalized in other situations.

## 3.2 Gantt Chart & Key Milestone

Timelines for FYP 1



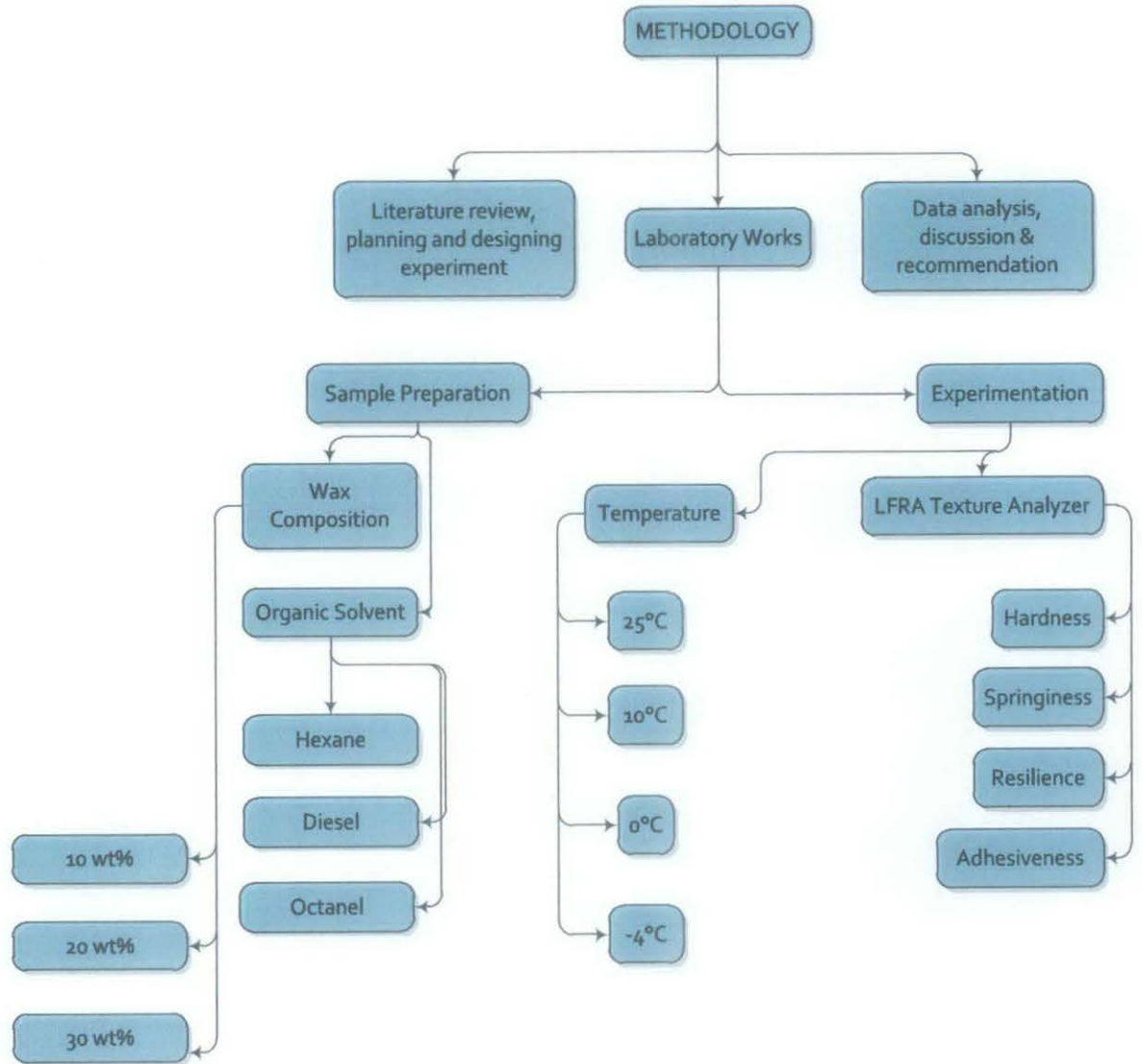
Timelines for FYP 2



Table 3.1: FYP II Milestone

No.	Action Item	Date	Note
1.	Briefing and update on students' progress	05/10/2011	Week 01
2.	Project work commences	03/10/2011	Week 02
3.	Submission of Progress Report	14/11/2011	Week 08
4.	Submission of Progress Report Marks	16/11/2011	Week 10
5.	Poster Exhibition / Pre-SEDEX	05/12/2011	Week 11
6.	SEDEX	13/12/2011	Week 12
7.	Submission of Final Report (CD Softcopy & Softbound)	19/12/2011	Week 13
8.	Delivery of Final Report to External Examiner / Marking by External Examiner	19/12/2011	Week 13
9.	Final Oral Presentation/Viva	27/12/2011	Week 14
10.	Submission of hardbound copies	06/01/2012	Week 15

### 3.2 Work Breakdown Mapping



### 3.3 Project Activity

This experiment will start with sample preparation. This is where the oil model will be built. Then it will undergoes LFRA Texture Analyzer to analyze the oil model texture after several calculation and mathematical expression and interpretations.

#### 3.3.1 Wax Characterization

Before the sample was begun to be prepared, the paraffin has to be characterized or finding its properties especially on the used paraffin wax. To determine the melting or freezing range the wax will be filled in a beaker to be heated preferably at lower heat. The first sign of liquid within the beaker is indicating the melting point of the wax. The melting point will be recorded until all the wax is melted and when the final solid melted, that is when the final range of melting temperature. The wax then cooled off to a room temperature and at the same time this melting range will be tested. First solid has been formed that is when the maximum range of melting point and will be recorded until all the wax has been solidified. The recorded temperature range will be compared and a melting range will be observed and decided. The wax density will be easily measured by measuring its volume and density. Below is step by step procedure for this wax characterization experimental work.



**Figure 3.1: Grinded wax**



**Figure 3.2: Moderate amount of grinded wax being heated**

1. Moderate amount of wax were cut small and filled in a 500 ml beaker after the beaker was weighed and then weighed again.
2. Then the wax was heated while its temperature being observed.
3. The temperature was recorded at the first sight of liquid formed from the solid wax.
4. The temperature then recorded back at a point when all wax was turned to liquid phase. All data are recorded as such per following table:

**Table 3.2: Wax properties**

<b>Properties of Wax</b>	<b>Data</b>
<b>Mass of Beaker</b>	(g)
<b>Mass of Beaker + Wax</b>	(g)
<b>Volume Wax</b>	(ml)
<b>Melting Point</b>	(°C)

5. From here the density of wax can be easily obtained.

### 3.3.2 Sample Preparation

The wax samples then will be grinded into smaller particle to ease liquefaction process. A 150 ml beaker is weighed and the electronic scale is set to 0 before the diesel will be poured into. The grinded waxes are carefully sprinkled into the beaker until it is measured precisely at 5 grams. The diesel is slowly and carefully poured into the particular beaker until measured precisely the electronic scale showing 50 grams. The excess diesel is drawn out by using laboratory dropper if necessary. The beaker opening is quickly wrapped with aluminum foil. The beaker is then heated up to in range of 50 degree Celsius on the laboratory hot plate until all the wax melted. If needed, a small hole will be penetrated with a glass rod and the solution is carefully stirred. The solution is waited until homogenous then cooled off to room temperature. Now it is a solution of 90 wt.% of wax and it is labeled as D90. The whole process is repeated according to the table 3.2. Again the whole process is repeated but now according to table 3.3. The following is the numerical step by step sample preparation procedures.

1. Several pieces of wax are grinded the solid wax into smaller particle.
2. A 150 ml beaker is weighed and the electronic scale set to 0 before the diesel will be poured into.
3. The grinded waxes are carefully sprinkled into the beaker until measured precisely at 45 grams.
4. The diesel is slowly and carefully poured into the particular beaker until the electronic scale shows 50 grams.
5. The excess diesel is drawn out by using laboratory dropper if necessary.
6. The beaker opening is quickly wrapped with aluminum foil.
7. The beaker is heated to 50 degree Celsius on the hot plate until all the wax melted.
8. If needed, a small hole will be penetrated with a glass rod and the solution is carefully stirred.
9. The solution is waited until homogenous then cools it off to room temperature.
10. It is now a solution of 10% wt. of wax. Label the solution as D10.



11. The above process are repeated according the following Table 3.3:

**Table 3.3: Wax-Diesel oil modeling with different wax composition**

<b>Solution (Wax-Diesel)</b>	<b>10% wt. of wax</b>	<b>20% wt. of wax</b>	<b>30% wt. of wax</b>
<b>Label</b>	D10	D20	D30
<b>Weight of grinded wax</b>	45 grams	40 grams	35 grams
<b>Weight of diesel</b>	5 grams	10 grams	15 grams

12. Now repeat step 6 to 14 for Wax-Octane solution according the following

Table 3.4:

**Table 3.4: Wax-Octane oil modeling with different wax composition**

<b>Solution (Wax-Octane)</b>	<b>10% wt. of wax</b>	<b>20% wt. of wax</b>	<b>30% wt. of wax</b>
<b>Label</b>	O10	O20	O30
<b>Weight of grinded wax</b>	45 grams	40 grams	35 grams
<b>Weight of acetone</b>	5 grams	10 grams	15 grams

13. Now repeat step 6 to 14 for Wax-Hexane solution according the following

Table 3.5:

**Table 3.5: Wax-Hexane oil modeling with different wax composition**

<b>Solution (Wax-Hexane)</b>	<b>10% wt. of wax</b>	<b>20% wt. of wax</b>	<b>30% wt. of wax</b>
<b>Label</b>	H10	H20	H30
<b>Weight of grinded wax</b>	45 grams	40 grams	35 grams
<b>Weight of acetone</b>	5 grams	10 grams	15 grams

### 3.3.3 Experimentation

In LFRA Texture Analyzer testing, the LFRA Texture Analyzer equipment have to be set up first that is including powering up the equipment, running the LFRA software and necessary steps need to be taken. The penetration depth is set at 5 mm located on both the device and software. The device mode is set to normal. Prior testing, the device is calibrated by ensuring that the pressurized value is zero. The probe type used would be TA10 where its rod diameter is much smaller then normally is since wax solution considered a heavy gel that acts partially like thermal-plastics. Basically following the information in the table 3.2.

**Table 3.6: LFRA Standard Settings**

<b>Properties</b>	<b>Value</b>
<b>Screen resolution</b>	2
<b>Probe Distance, mm</b>	5.00
<b>Probe Speed, mm/s</b>	2.00
<b>Cycle Type</b>	Normal
<b>Calibration factor</b>	768003.00
<b>System type</b>	2.00
<b>Probe Type</b>	TA10
<b>Load Type</b>	Comp

1. The LFRA Texture Analyzer equipment is powered on
2. The computer is ran and so as the LFRA software
3. The penetration depth is set at 10mm located on the device and software
4. The device mode is set to cycle
5. The device is calibrated by ensuring that pressurized value is zero
6. A sample is positioned (with the beaker) on the testing platform
7. The device is ran and waited until several cycles before stop the experiment
8. The graph envelope is extracted and other readings such as hardness, adhesiveness, adhesive force and resilience will be mathematically calculated. This will be a data at room temperature (25 °C)
9. Step 5 to 8 is repeated at lower set of temperatures by chilling the sample a little bit lower than the desired temperatures (10°C, 0°C & - 4°C) in a laboratory chiller before putting the sample on the testing platform. Make sure that the experiment done swiftly and yet carefully
10. Step 5 to 9 is repeated with all other samples as in the table 3.3, 3.4 and 3.5
11. The graph is plotted with desired properties against different solutions at a single temperature, against different temperature at a single solution
12. The graphs interpreted and correlated between them

### **3.4 Tools Required**

Here are some tools that required for the experiments. Tools are divided into three categories which is equipment, chemicals and apparatus. Equipment is the set of articles or physical resources serving to equip a person or thing as the implements used in an operation or activity. There are 4 equipment are listed and they are

laboratory electronic scale, laboratory hot plate, laboratory chiller and most important is LFRA Texture Analyzer. There are also three chemicals that required for this project. The chemicals are substances with a distinct molecular composition that is produced by or used in a chemical process. After some calculations with included margin of errors, 5 L of common hexane, 5 L of common diesel and 5 kg of paraffin wax are estimated to be used. Apparatus are usually known as laboratory utensils. There are several of apparatus that required for this project. The apparatus are listed down in the following after equipment and chemicals.

#### **3.4.1 Equipment**

1. Laboratory Electronic Scale
2. Laboratory Hot Plate
3. LFRA Texture Analyzer
4. Laboratory Chiller

#### **3.4.2 Chemicals**

1. 5 liters of Petrol
2. 5 liters of Hexane
3. 5 kilograms of Paraffin Wax

#### **3.4.3 Apparatus**

1. At least 3 beakers of 250 ml
2. At least 2 beakers of 500 ml
3. A spatula
4. A glass rod
5. A laboratory thermometer
6. A laboratory dropper
7. A sheet or roll of aluminum foil
8. A 100 ml measuring cylinder
9. Labeling stickers

## CHAPTER 4: RESULTS AND DISCUSSIONS

### 4.1 Wax Characterization

The results of wax characterization are recorded in Table 4.1. It is understandable that the melting point of wax is not at a single point like water that is 100°C. This is due to the wax composition itself since paraffin wax consists of several carbon chain components that are usually above 22 carbon chain molecules. The density is obtained by dividing mass of wax with volume of wax. The range of melting point plays a very big role in the experimental procedures.

Table 4.1: Results of Wax Characterization

Properties of Wax	Data
Mass of Beaker	203 <i>g</i>
Mass of Beaker + Wax	457.27 <i>g</i>
Volume Wax	345 <i>ml</i>
Melting Point	43°C – 50°C
Density	0.737 $\frac{g}{ml}$

### 4.2 LFRA Texture Analysis

Here are few samples the typical graphs produced by a machine called LFRA Texture Analyzer for the provided samples. Know that the speed of probe is constant at  $2 \frac{mm}{s}$ , probe type is constant so as its diameter and the depth of penetration is constant as well at 5 *mm*. Note that some of the oil modeled is in liquid form at certain temperature, composition and solvent type. Therefore LFRA TA is unable to produce any result. The “unsuccessful” oil models are:

1. Hexane-wax 10 wt.% at any designated temperatures
2. Hexane-wax 20 wt.% at 0, 10 and 25 degree Celsius
3. Hexane-wax 30 wt.% at 25 degree Celsius
4. Octane-wax 20 & 30 wt.% at 25 degree Celsius
5. Octane-wax 10 wt.% at any designated temperatures
6. Diesel-wax 10 wt.% at 25 degree Celsius

From Figure 4.1, is one of graph produced by LFRA for a Hexane-wax solution at  $-4^{\circ}\text{C}$ . By the graph we can deduce that the solution is in mixture of liquid and solid or partially solidified. The unevenness of plateau is caused by variations in the firmness or toughness of the particles that are passing through the annulus zone at any particular thus indicating mixture of liquid and solid. Initially the oil model is deformed and compressed to pack more and more tightly into diminishing space available under the descending plunger; there is almost no rupture or breaking of the oil model. At approximately between the slopes is changing from initially, the solution is packed solid and liquid begins to be pressed out from the solution. Soon afterwards the pack is solid except for small amounts of entrapped air, and the forces increases steeply pressing out more liquids. At the highest peak or point, the oil model begins to rupture and flow up through the annulus and this process continues to a point where the compressing platen reverses direction and the force falls to zero.

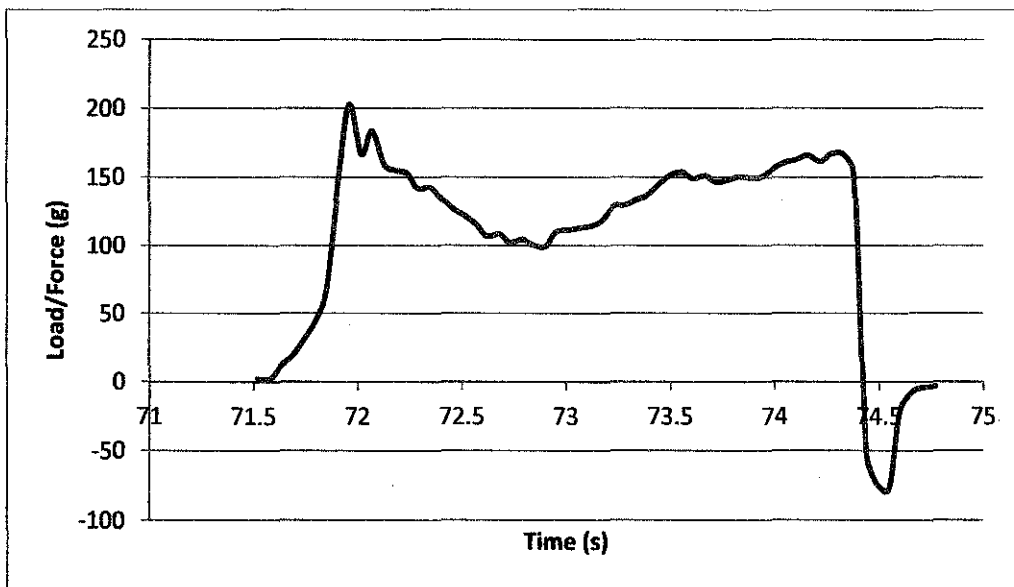


**Figure 4.1: Wax-Hexane 30wt% solution at  $-4^{\circ}\text{C}$**

At the bio-yield point indicates the force necessary to begin the process of extrusion and the plateau shows the force needed to continue extrusion. At the highest slope between initial compression and bio-yield point represents the increasing force being applied to an almost incompressible mixture of solids and liquid.

The plateau shows decrement at first indication some shearing resistance combined with some extrusion and possibly adhesion of the sample to test cell then increases as

extrusion proceed showing further compression if the sample in addition to various amounts of adhesion, extrusion and shearing.

#### 4.2.1 Effect of Solvent

From the empirical scale, force can be dominated as in unit of gram. Figure 4.2 shows a distinctive trending that is as hardness increases almost exponentially as the number of carbon chain in solvent as in higher carbon chain value of solvent gives higher hardness in exponential increment. This trending can be observed to any type of solvents, at any temperatures and at any composition. This is as discussed before the oil model becomes harder as the temperature decreases the energy of molecule diminished and the bonds between them are strengthened.

Figure 4.3 does not give an absolute trending. Generally it gives a polynomial curve but as temperature raises the curve become lesser and at temperature of 10°C it becomes almost linear to adhesive force toward the carbon chain value of solvent. Thus by increasing the temperature will make the trending much more predictable.

Using trapezoidal rule as a function of are under the curve gives Figure 4.4 and 4.5 that indicating adhesiveness and resilience. Unfortunately it does not give any pattern or trending between solvents only chaotic plots of data can be observed.

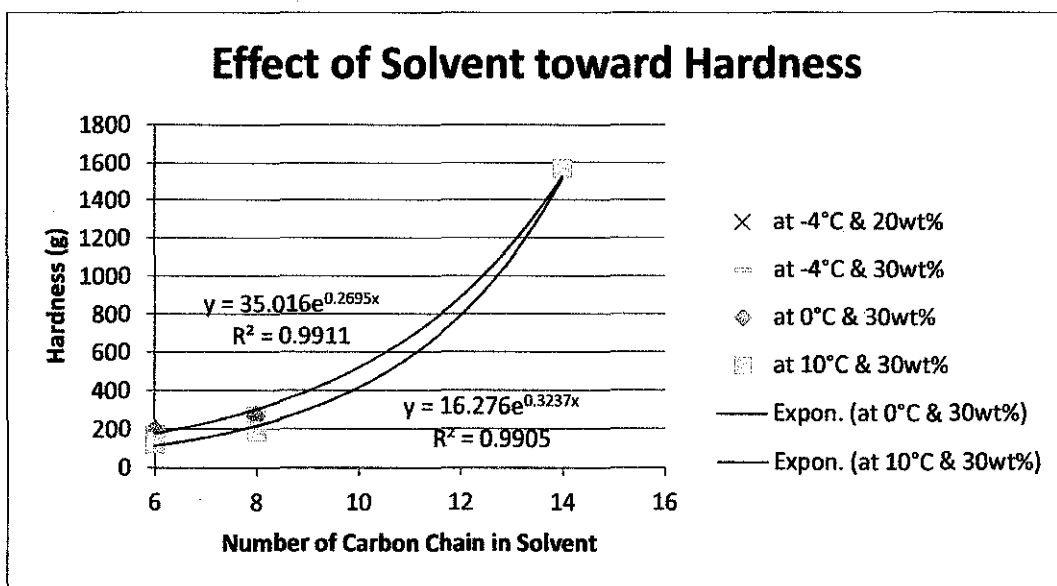
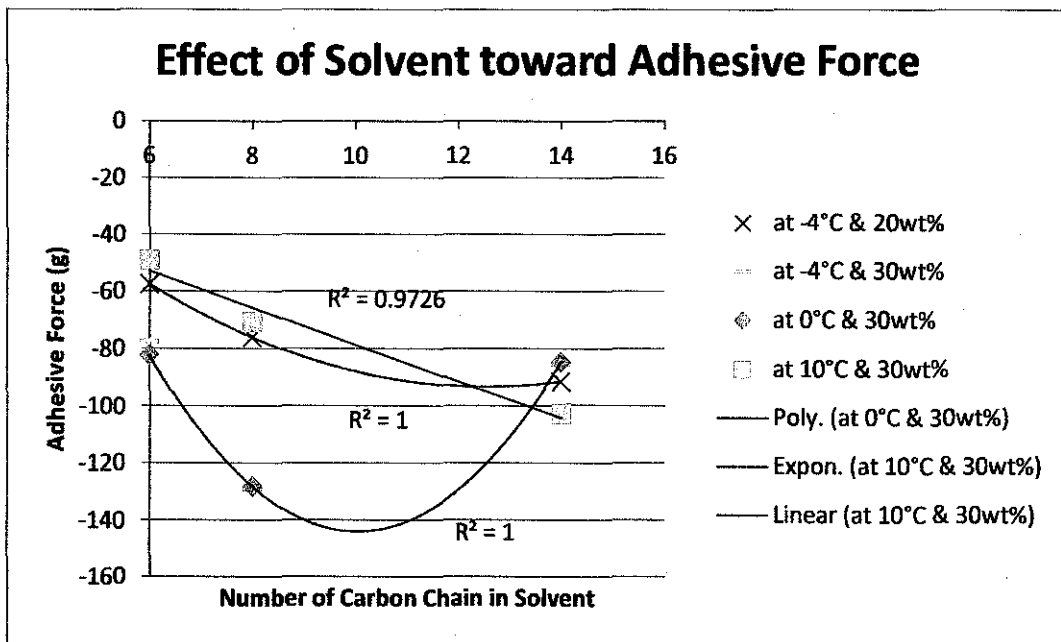
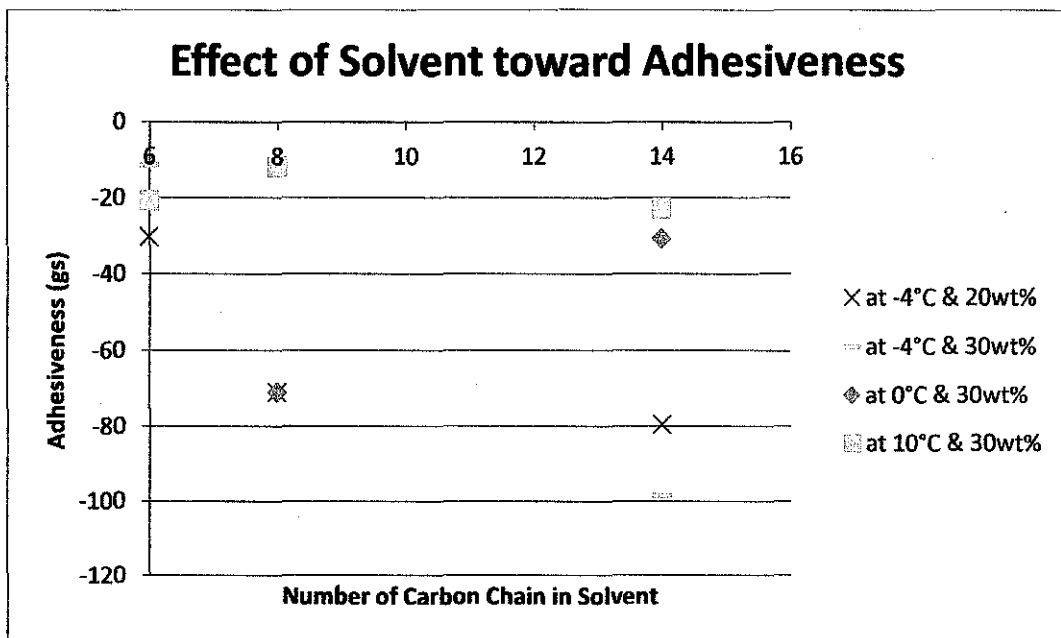


Figure 4.2: Effect of Solvent toward Hardness



**Figure 4.3: Effect of Solvent toward Adhesive Force**



**Figure 4.4: Effect of Solvent toward Adhesiveness**

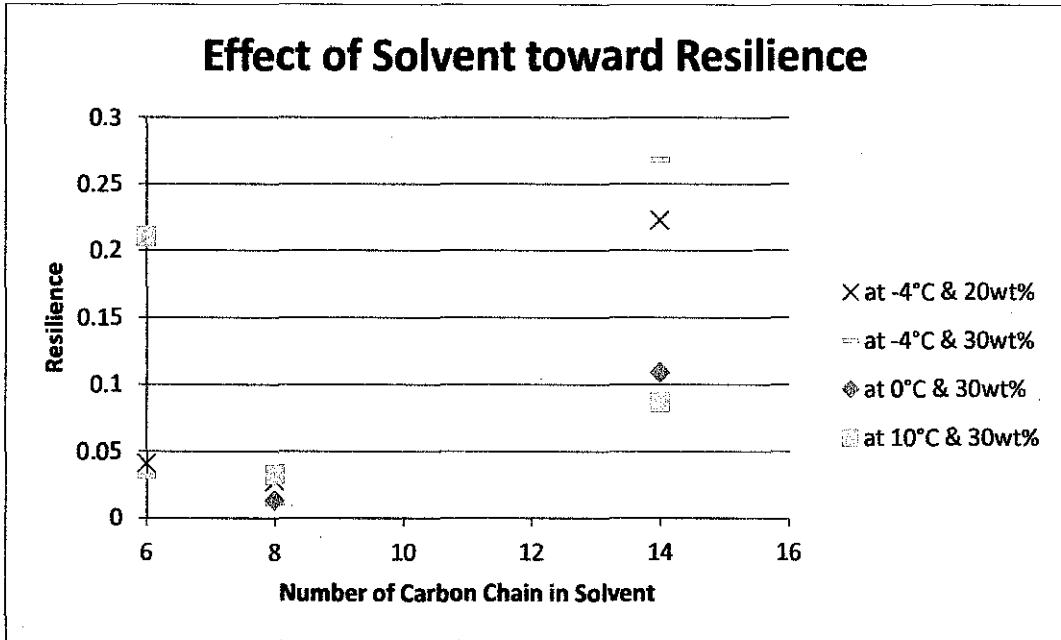


Figure 4.5: Effect of Solvent toward Resilience

#### 4.2.2 Effect of Temperature

Figure 4.6 indicate that hardness decrease linearly as temperature increases. It makes sense to a basic chemistry concept that when temperature rise give energy to molecules gives more vibrations that weaken the bonds between them.

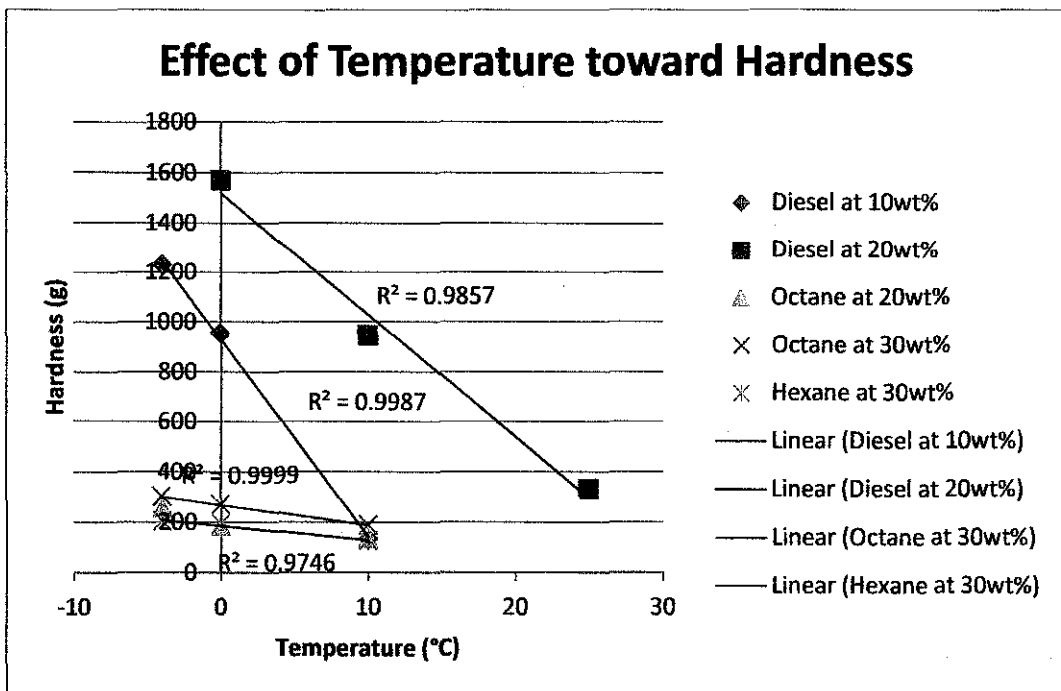


Figure 4.6: Effect of Temperature toward Hardness



Figure 4.6 also indicate that the lower wt.% composition of wax gives lower slope means the hardness change are smaller or less sensitive compared to those have higher wax content. This trend can also be observed to the lower carbon chain solvents.

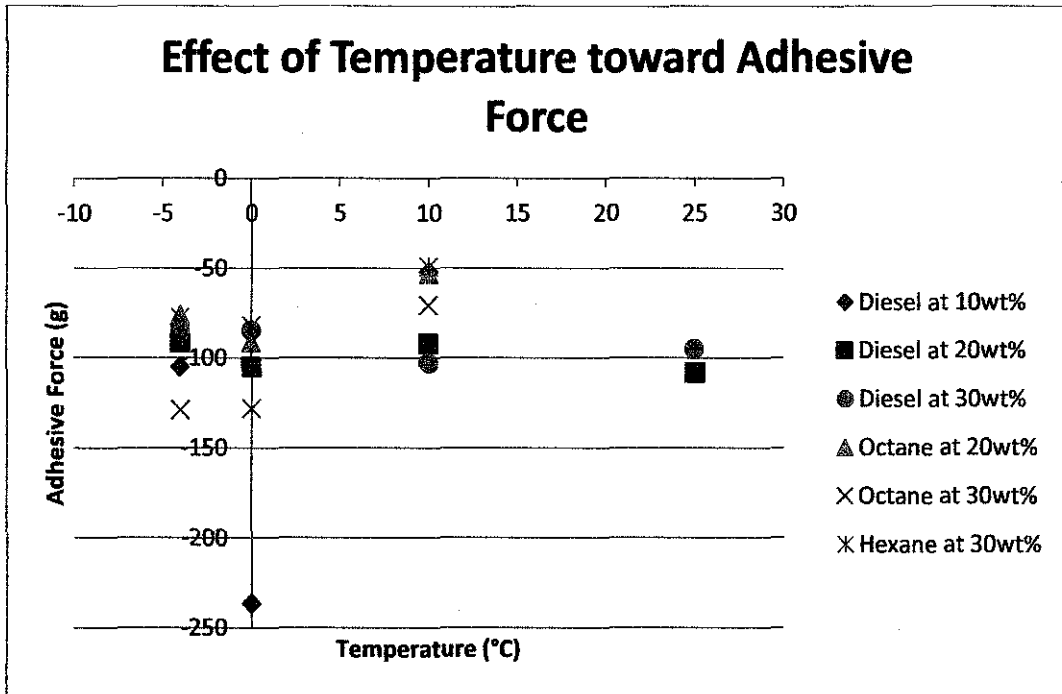


Figure 4.7: Effect of Temperature toward Adhesive Force

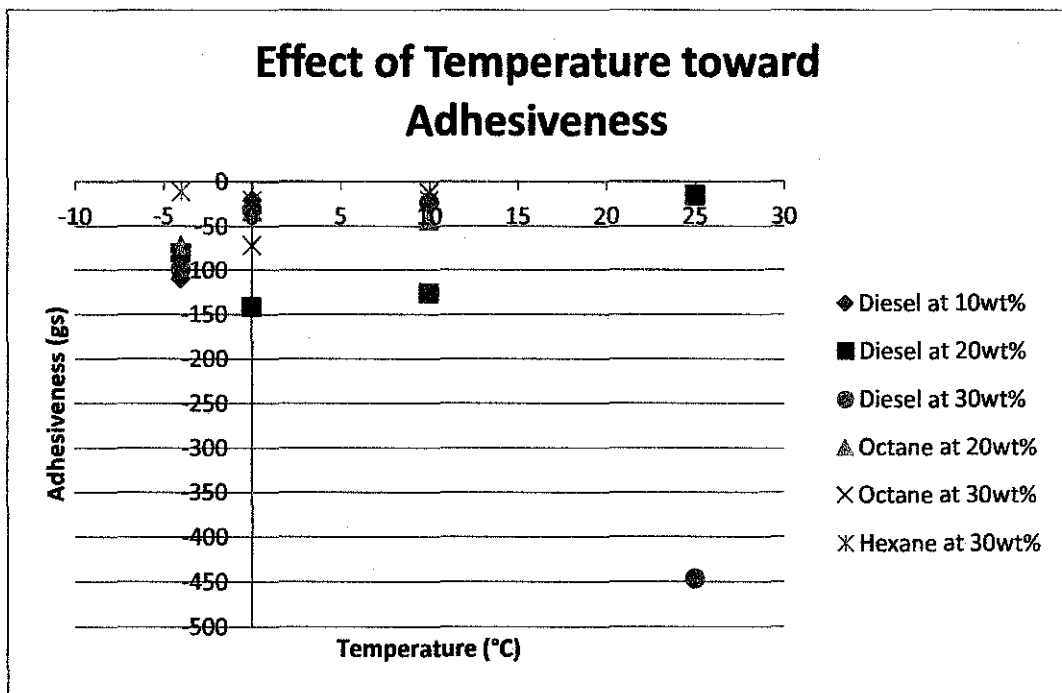


Figure 4.8: Effect of Temperature toward Adhesiveness

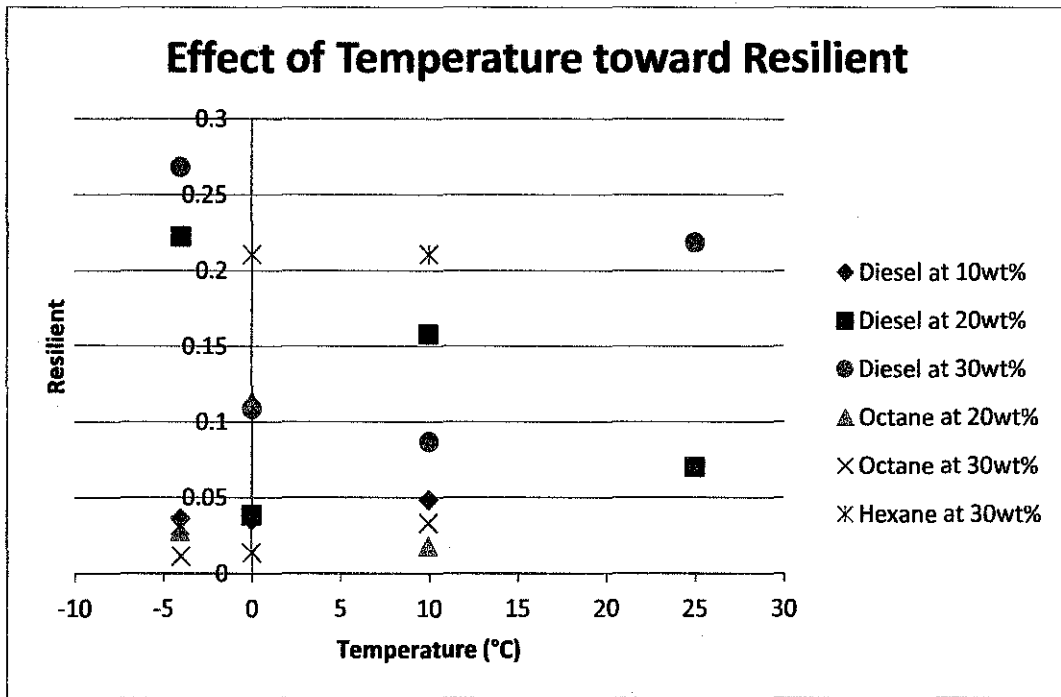


Figure 4.9: Effect of Temperature toward Resilient

#### 4.2.3 Effect of Composition

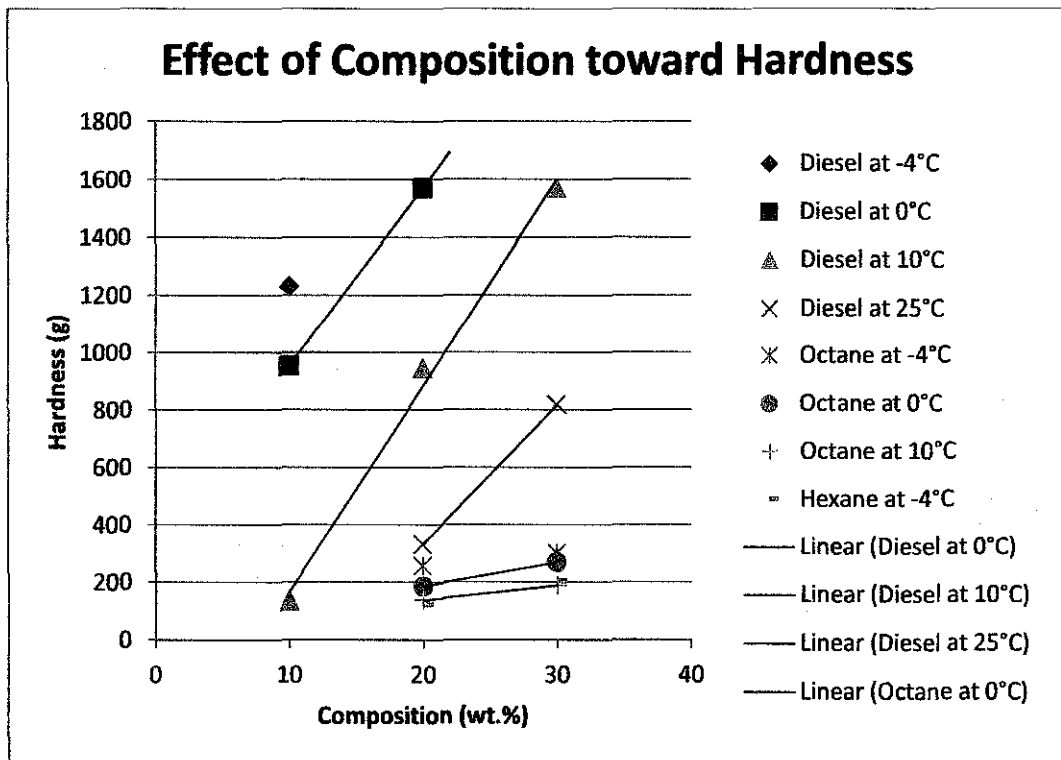


Figure 4.10: Effect of Composition toward Hardness

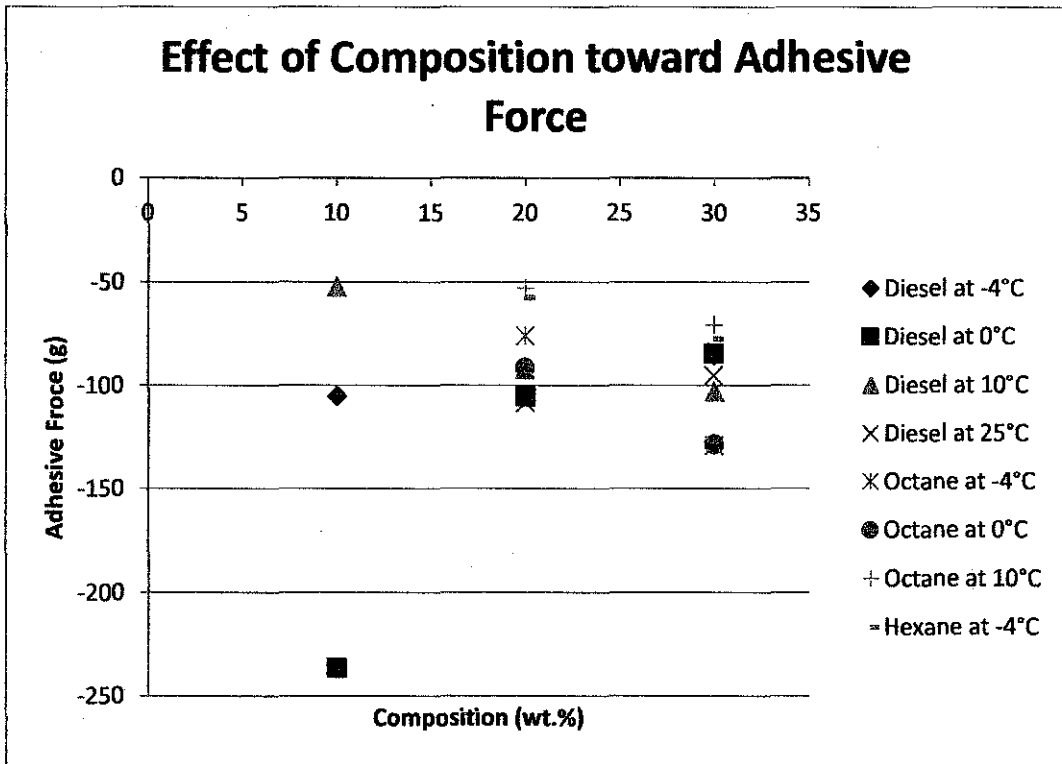


Figure 4.11: Effect of Composition toward Adhesive Force

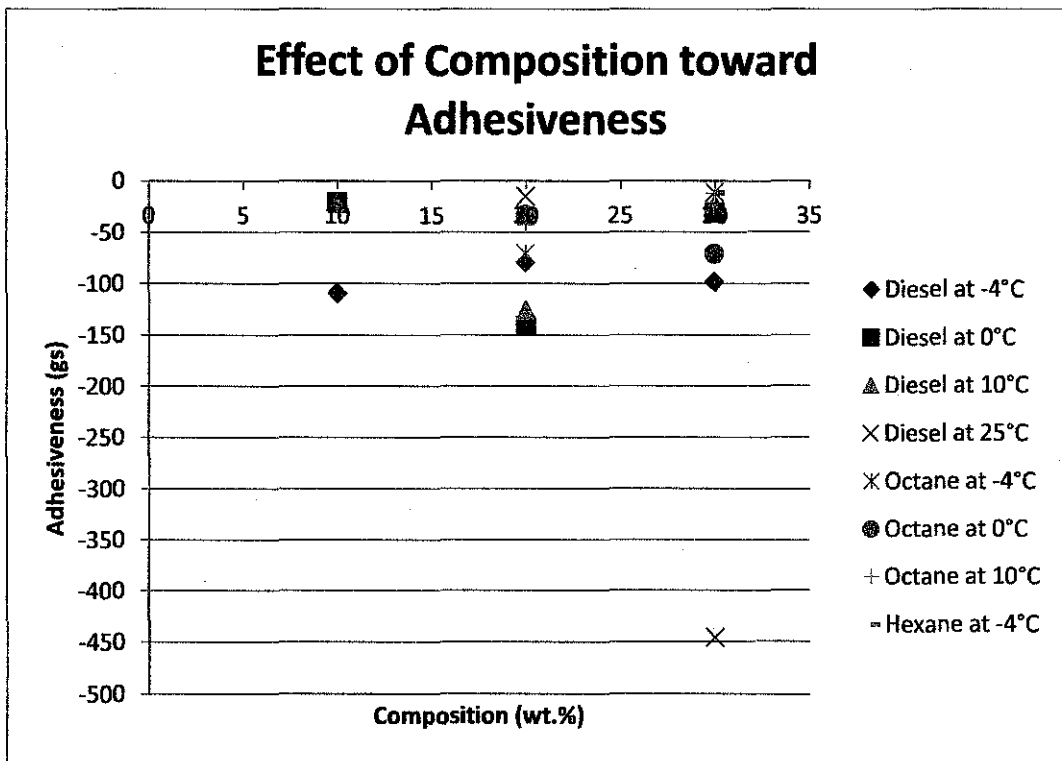
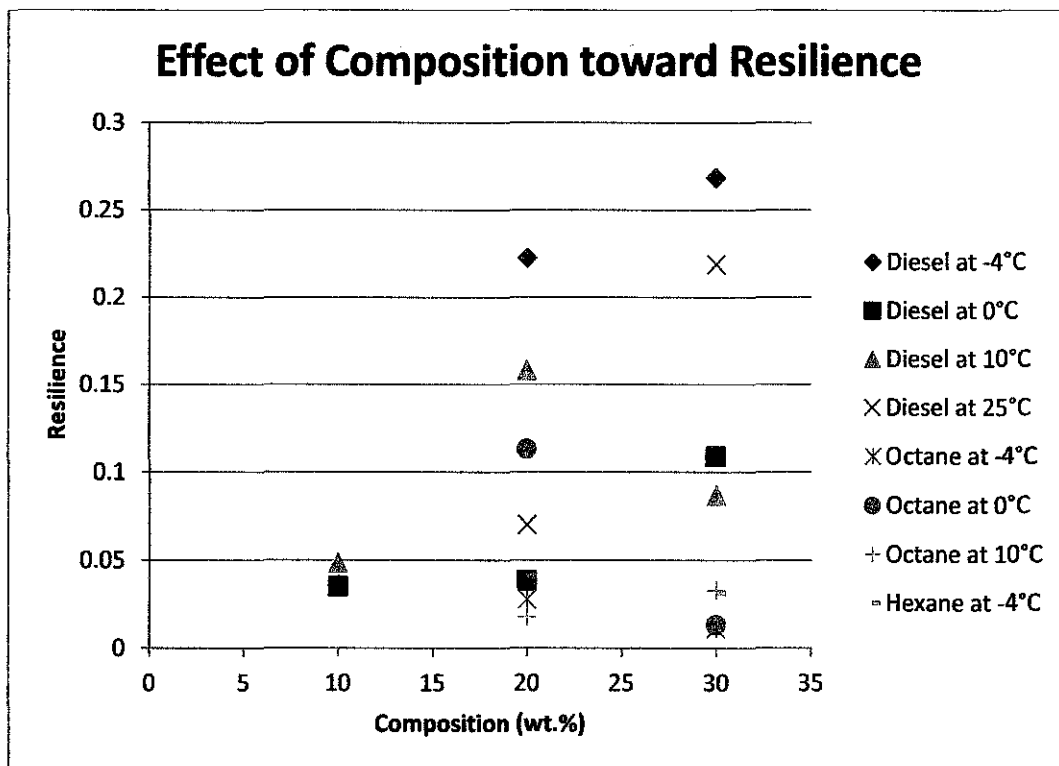


Figure 4.12: Effect of Composition toward Adhesiveness



**Figure 4.13: Effect of Composition toward Resilience**

The effect of composition is similar in temperature in term of hardness. We can see the trending is linear where higher composition of wax gives higher hardness. Other properties give erratic and chaotic trending however if observed adhesiveness and adhesive force for both effect of temperature and composition it show a constant or similar results at any given conditions of temperatures, compositions and solvents. It distributed within the range of 0 to -150 (gs). This may promote that adhesiveness and adhesive force does not change much as temperature change or wax content changed. Resilience for both effects seems chaotic but if observed closely enough, it never distributed out of range 0 to 0.3 same goes to solvent effects.

## **CHAPTER 5: CONCLUSION AND RECOMMENDATION**

Study of wax characterization and texture will contribute to a better understanding of the ability to predict wax deposition thus the avoidance or remediation of wax deposition for flow assurance especially in oil and gas industries. The experimental work for the project is still ongoing. From the result of this project, we will be able to study the wax characterization and wax texture properties from LFRA Texture Analyzer and the testing method and principle behind it. To achieve the aim for this project, we start with oil modeling by varying three different wax compositions which is 10 wt.%, 20 wt.% and 30 wt.% in three different organic solvents that have been decided that is common diesel, hexane and octane. The oil models will undergo a texture analysis using LFRA Texture Analyzer. From here specific information such as hardness, adhesive force, resilience and adhesiveness will be able to determine. By the results, a correlation between wax texture and wax content shall be able to deduce with certain investigation and analysis.

The results show that only hardness of the oil model gives a specific trending. Effect of solvent gives exponentially growth trending between hardness while effect of temperature gives linear declining trending between hardness and effect of composition gives linear increment of hardness. Solvent effect toward adhesive force suggesting a polynomial curve but as temperature rises or wax composition decreases it tends to becoming linear. No specific correlation can be made for adhesiveness and resilience to any effects. It is also observed that adhesiveness and adhesive force are closely related as they seem to fall into a certain range or to say much consistent than other parameters.

In the future work plan, this project could expand its parameters by using cycle mode in LFRA TA. All the listed parameters listed in the literature review could be obtained. Another is by introducing shear force in this experiment so that it will become more “pipe-like” condition. A thorough research on crude oil at first point it comes out and throughout the pipelines should be done as well. Matching the possible temperature will definitely give a much more accurate and refined correlations. Flow-ability of wax solution should be a great focus and ability to forecast it under certain conditions and parameters will be a major help.

## REFERENCES

- Aiyejina, A., Chakrabarti, D. P., Pilgrim, A., & Sastry, M. (2011). Wax formation in oil pipelines: A critical review. *International Journal of Multiphase Flow*, XXXVII, 671-694.
- Ashenville Oil Company. (2002). Paraffin Waxes.
- Avrami, M. (1939). Kinetics of phase change I: General theory. *Journal of Chemical Physics*, VII, 1103-1112.
- Avrami, M. (1940). Kinetics of phase change II: Transformation-time relations for random distribution of nuclei. *Journal of Chemical Physical*, VIII, 212-224.
- Azevedo, L. F., & Teixeira, A. M. (2003). A critical review of the modeling of wax deposition mechanisms. *Petroleum Science Technology*, XXI, 393-408.
- Bhattacharyya, A. R., Sreekumar, T. V., Liu, T., Kumar, S., Ericson, L., Hauge, R. H., et al. (2003). Crystallisation and orientation studies in polypropylene/single wall carbon nanotube composite. *Polymer*, XLIV, 2373-2377.
- Bourne, M. C. (2002). *Food Texture and Viscosity: Concept and Measurement* (2nd ed.). New York, Geneva, United States of America: Academic Press.
- Burger, E. D., Perkins, T. K., & Stiegler, J. H. (1981). Studies of wax deposition in the trans alaska pipeline. *SPE: Journal of Petroleum Technology*, XXXIII, 1075-1089.
- Campos, R. J., Litwinenko, J. W., & Marangoni, A. G. (2003). Fractionation of milk fat by short-path distillation. *Journal of Dairy Science*, LXXXVI, 735-745.
- Caze, C., Devaux, E., Crespy, A., & Cavrot, J. P. (1997). A new method to determine the Avrami exponent by D.S.C. studies of non-isothermal crystallisation from the molten state. *Polymer*, XXXVIII(3), 497-502.
- Chen, D. Z., He, P. S., & Pan, L. J. (2003). Cure kinetics of epoxy-based nanocomposites analysed by Avrami theory of phase change. *Polymer Testing*, LXXXVI, 689-697.
- Chevron Lubricants. (2002). Chevron Refined Waxes.
- Connor, M. T., Gutierrez, M. G., Rueda, D. R., & Calleja, F. J. (2003). Cold crystallisation studies on PET/PEN blends as revealed by microhardness. *Journal Material Science*, XXXII.
- Correra, S., Fasano, A., Fusi, L., & Merino-Garcia, D. (2007). Calculating deposit formation in the pipelining of waxy crude oils. *Meccanica*(XLII), 149-165.
- Cote, A., & Linville, J. (1991). *Fire Protection Handbook* (17th ed.). Quincy, MA: National Fire Protection Association.
- Ekweribe, C. K. (2008). Quiscent Gelation of Waxy Crudes and Restart of Shut-in Subsea Pipelines. *MS Thesis*.

- Evans, U. R. (1945). The laws of expanding circles and spheres in relation to lateral growth of surface films and the grain size of metals. *Journal of the Chemical Society, Faraday Transaction, XLI*, 365-374.
- Exxon Mobil Corporation. (August 13, 1999). *Fully Refined Paraffin Waxes*. Product Information Bulletin DG-4A.
- Fasano, A., Fusi, L., & Correra, S. (2004). Mathematical models for waxy crude oils. *Meccanica, XXXIX*, 441-482.
- Fiszman, S. M., & Damasio, M. H. (2000, April). Intrusmental Measurement of Adhesiveness in Solid and Semi-solid Foods. *Texture Studies, XXXI(1)*, 69-91.
- Fusi, L. (2003). On the stationary flow of a waxy crude oil with deposition mechanisms. *Nonlinear Analysis, 507-526*.
- Gaydon, A. a. (1979). *Flames: Their Structure, Radiation and Temperature* (4th ed.). New York: John Wiley and Sons.
- Hay, J. N. (1971). Application of the modified Avrami equations to polymer crystallisation kinetics. *British Polymer Journal, III(2)*, 75-82.
- Himran, S., & Suwono, A. (1994). Characterization of Alkanes and Paraffin Waxes for Application as Phase Change Energy Storage Medium. *Energy Sources, XVI*, 117-128.
- Hotwatt Inc. (n.d.). *Properties of Non-Metallic Solids*. Retrieved June 27, 2011, from Wattage Calculation Formulas - Paraffin Melting: <http://www.hotwatt.com/>
- Huang, X., Terech, P., Raghavan, S. R., & Weiss, R. G. (2005). Kinetics of 5 $\alpha$ -cholestan-3 $\beta$ -yl N-(3-naphthyl)carbamate/n-alkane organogel formation and its influence on the fibrillar network. *Journal of the American Chemical Society, CXXVII(12)*, 4335-4344.
- Hunt, E. B. (1962). Laboratory study of paraffin deposition. *SPE: Journal of Petroleum Technology, 1259-1269*.
- Ismail, L., Westacott, R. E., & Xiongwei, N. (2007, April 14). On the effect of wax content on paraffin wax deposition in a batch oscillatory baffled tube apparatus. *Chemical Engineering Journal, 205-213*.
- Kawanaka, S., Park, S. J., & Mansoori, G. A. (1991, May). Organic deposition from reservoir fluids. *SPE Reservoir Engineering Journal, 185-192*.
- Kirk-Othmer. (1999). *Encyclopedia of Chemical Technology* (3rd ed.). New York: John Wiley & Sons.
- Kyeongseok, O., Mark, J., Pankaj, T., Jules, M., & Millind, D. (2006). Partial Recovery of Wax Gel Strength: Quantitative and Qualitative Analyses. *University of Utah, Salt Lake City*.

- Leiroz, A. T., & Azevedo, L. F. (2005). Studies on the mechanisms of wax deposition in pipelines. *Offshore Technology Conference*. Houston: Offshore Technology Conference.
- Li, W., Kong, X., Zhou, E., & Ma, D. (2005). Isothermal crystallisation kinetics of poly(ethylene terephthalate)-poly(ethylene oxide) segmented copolymer with two crystallising blocks. *Polymer*, *XLVI*, 11655-11663.
- Litwinenko, J. W., Singh, A. P., & Marangoni, A. J. (2004). Effect of glycerol and Tween 60 on the crystallisation behaviour, mechanical properties, and microstructure of plastic fat. *Crystal Growth & Design*, *IV*(1), 161-168.
- Lopez-da-Silva, J. A., & Coutinho, J. A. (2007). Analysis of the isothermal structure development in waxy crude oils under quiescent condition. *Energy Fuels*, *XXI*, 3612-3617.
- Lu, M. G., Shim, M. J., & Kim, S. W. (1998). Curing behaviour of unsaturated polyester system analysed by Avrami equation. *Thermochimica Acta*, *CCCXXIII*, 37-42.
- Luo, H., Sietsma, J., & Zwaag, V. d. (2004). Effect of inhomogeneous deformation on the recrystallisation kinetics of deformed metals. *ISIJ International*, *XLIV*(11), 1931-1936.
- Merino-Garcia, D., Margarone, M., & Corraera, S. (2007). Kinetics of waxy gel formation from batch experiments. *Energy Fuels*, *XXI*, 1287-1295.
- Merriam-Webster Incorporated. (2011). *Dictionary and Thesaurus: Merriam-Webster*. Retrieved June 27, 2011, from Merriam-Webster: <http://www.merriam-webster.com/dictionary/paraffin>
- Mozes, Y. G. (1982). *Paraffin products: Properties, technology, applications*. New York: Elsevier Scientific Publishing.
- Nigmatullin, P. A. (1997). Purifying and Deoiling Slack Wax for the Manufacture of Paraffin Waxes. *Chemistry and Technology of Fuels and Oils*, 18-19.
- North American Mfg. Co. (1999). *North American Combustion Handbook* (2nd ed.). Cleveland: OH.
- Pal, S., & Nandi, A. K. (2005). CocrySTALLISATION mechanism of poly(3-alkyl thiophenes) with different alkyl chain length. *Polymer*, *XLVI*, 8321-8330.
- Paso, K. G. (2005). Paraffin Gelation Kinetics. *PhD Dissertation*.
- Peleg, M. (1977, September). Operational Conditions and the Stress-Strain Relationship of Solid Foods - Theoretical Evaluation. *Texture Studies*, *VIII*(3), 283-295.
- Pereira, R. P., & Rocco, A. M. (2005). Nanostructure and crystallisation kinetics of poly(ethylene oxide)/poly(4-vinylphenol-co-2-hydroxyethyl methacrylate) blends. *Polymer*, *XLVI*, 12493-12502.
- Sanderson, J. (1997). *Candle Fires* (4th ed., Vol. V). Fire Findings.



- Sciencelab.com Inc. (2010, November 1). Material Safety Data Sheets (MSDS) for Paraffin Wax. *MSDS*. Houston, Texas, United States of America.
- Sharples, A. (1966). Overall kinetics of crystallisation. In A. Sharples, *Introduction to Polymer Crystallisation* (pp. 44-59). London: Edward Arnold Ltd.
- Shell Lubricant. (October 2000). *Shell Paraffin and Microcrystalline Waxes: SHELLWAX and SHELLMAX*. Technical Bulletin.
- Singh, P., Venkatesan, R., & Fogler, H. S. (2000). Formation and aging of incipient thin film wax-oil gels. *AIChE Journal*, *XLVI*(5), 1059-1074.
- Solaimany, N. A., Dabir, B., & Islam, M. R. (2005). Experimental and mathematical modeling of wax deposition and propagation in pipes transporting crude oil. *Energy Source*, *XXVII*.
- Sperling, L. H. (1986). Kinetics of crystallization. In L. H. Sperling, *Introduction to Physical Polymer Science* (pp. 177-191). New York: John Wiley and Sons.
- Szczesniak, A. S., & Hall, B. J. (1975, March). Application of the General Foods Texturometer to Specific Food Products. *Texture Studies*, *VI*(1), 117-138.
- Townsend, D. (October 1999). *Fires Associated with the Use of Night Light Candles (Tea Lights)*. London: London Fire Brigade.
- Voisey, P. W. (1971, May). Modernization of Texture Instrumentation. *Texture Study*, *II*(2), 129-195.
- Wang, X., & Vlassak, J. J. (2006). Crystallization kinetics of amorphous NiTi shape memory alloy thin film. *Scripta Materials*, *LIV*(5), 925-930.

## APPENDIX

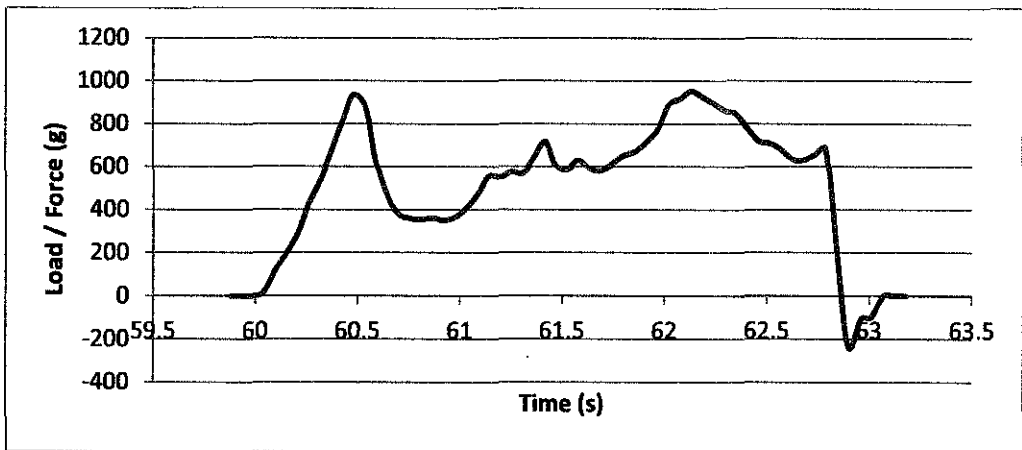


Figure 1: Diesel at 10 wt.% of wax at -4°C

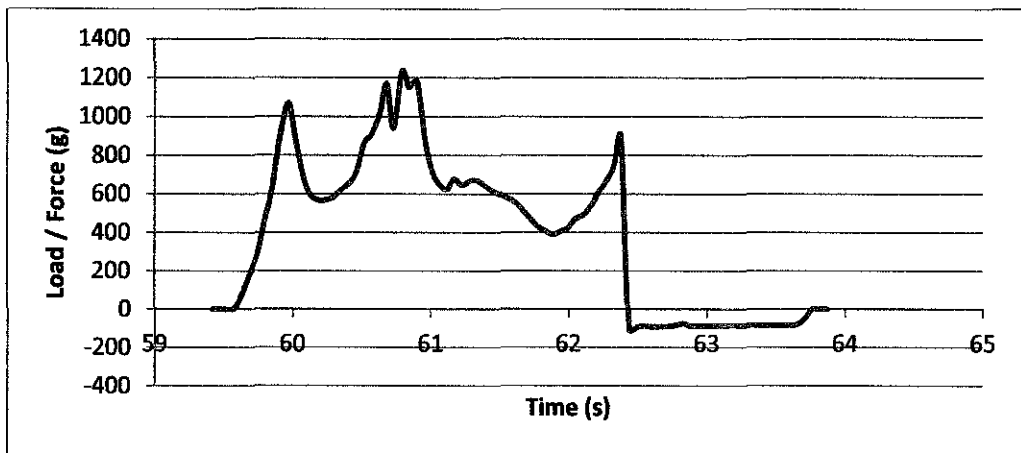


Figure 2: Diesel at 10 wt.% of wax at 0°C

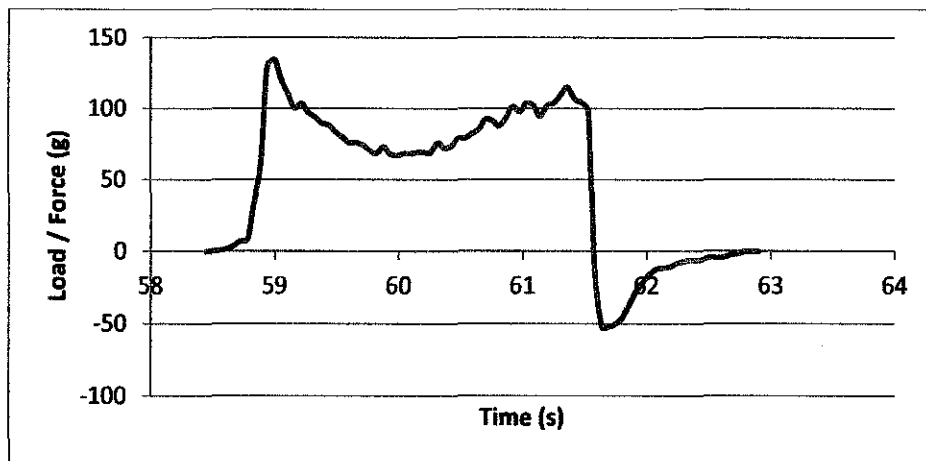
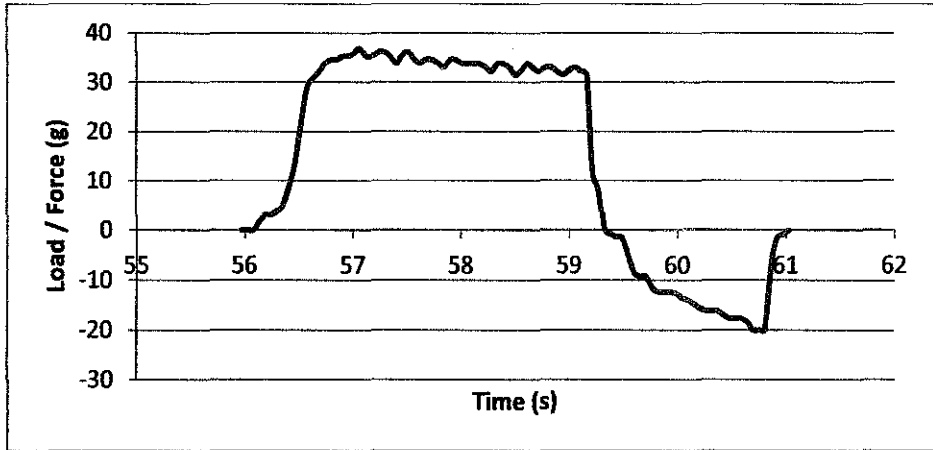
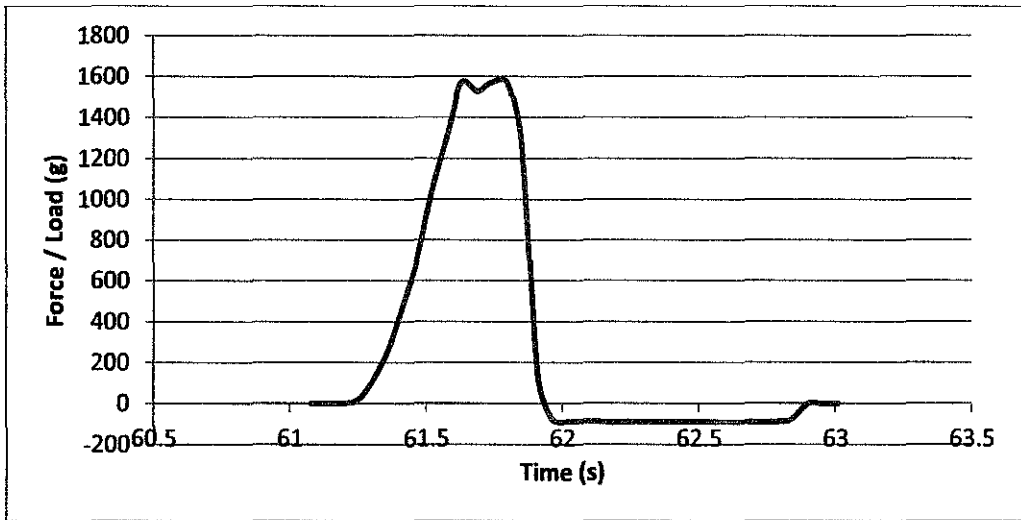


Figure 3: Diesel at 10 wt.% of wax at 10°C



**Figure 4: Diesel at 10 wt.% of wax at 25°C**



**Figure 5: Diesel at 20 wt.% of wax at -4°C**

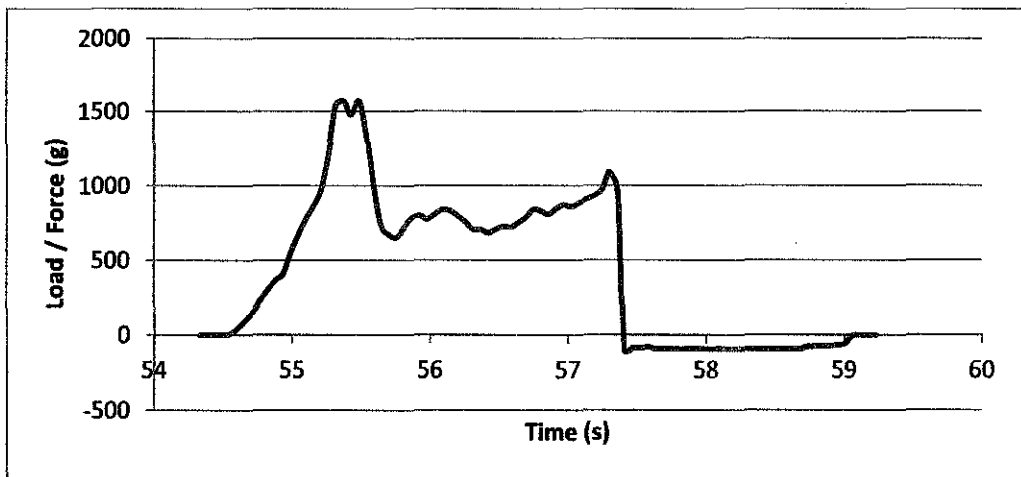


**Figure 6: Diesel at 20 wt.% of wax at 0°C**

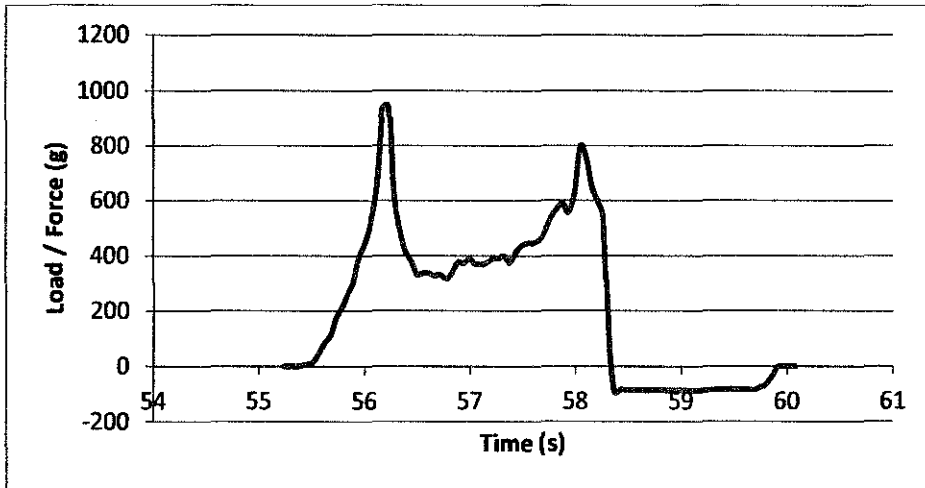


**Figure 7: Diesel at 20 wt.% of wax at 10°C**

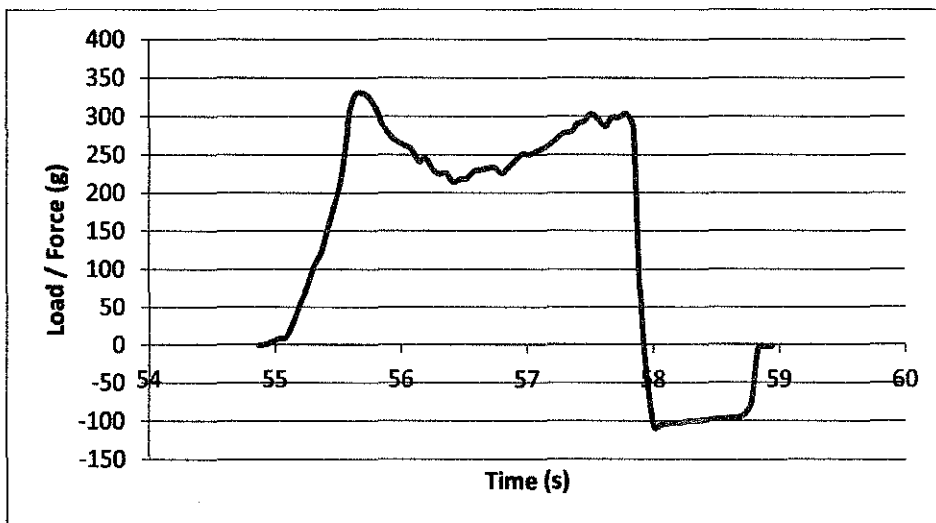


**Figure 7: Diesel at 20 wt.% of wax at 10°C**

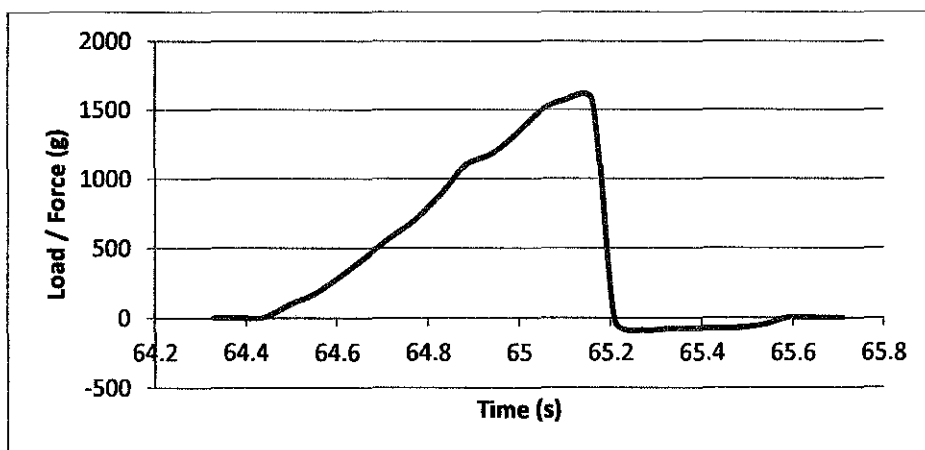


**Figure 8: Diesel at 30 wt.% of wax at -4°C**

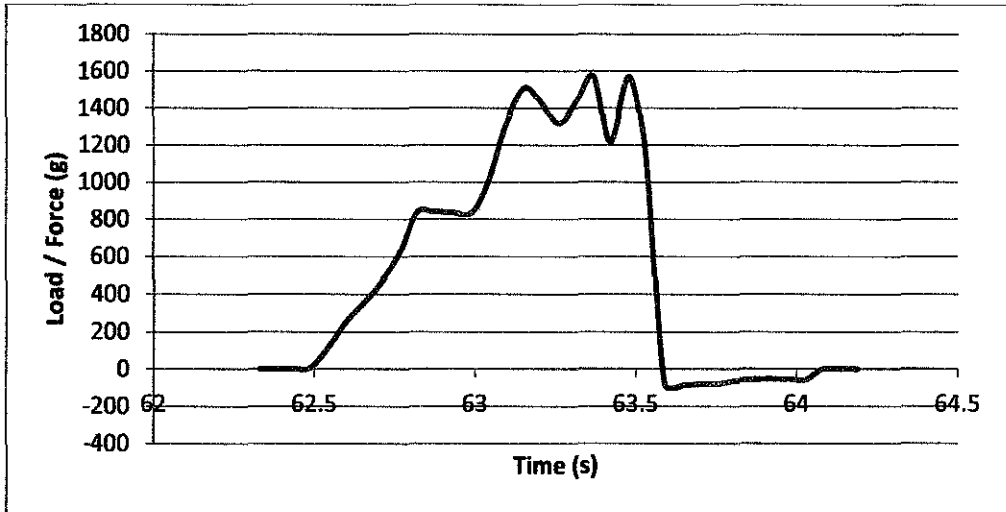


**Figure 9: Diesel at 30 wt.% of wax at 0°C**

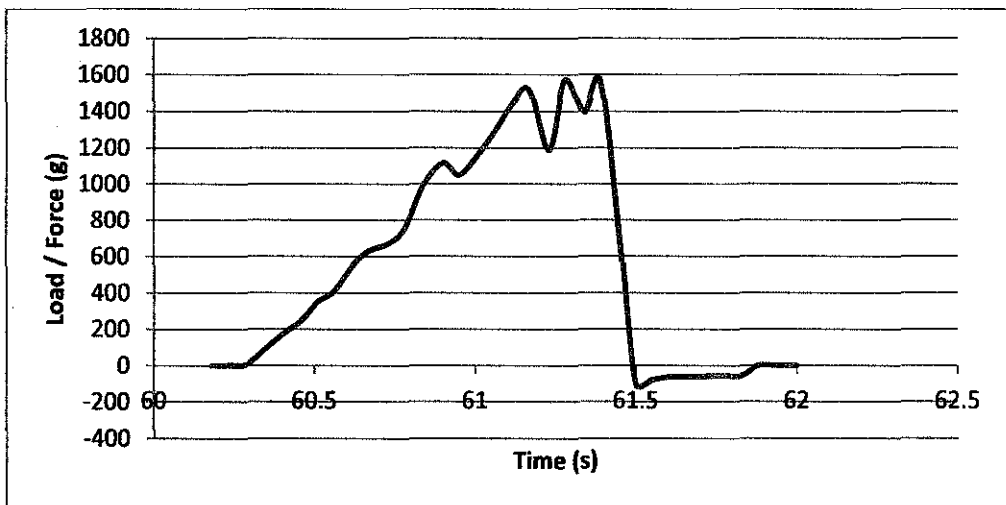


**Figure 10: Diesel at 30 wt.% of wax at 10°C**

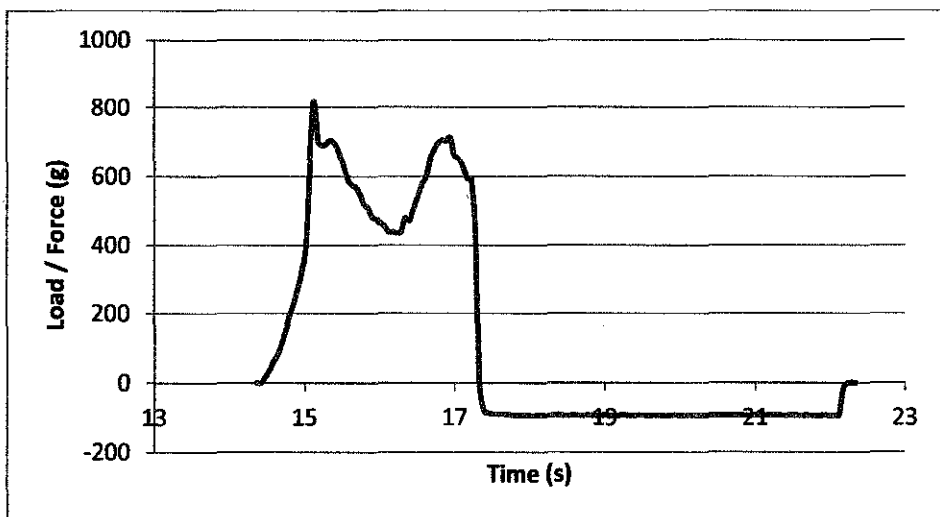


**Figure 11: Diesel at 30 wt.% of wax at 25°C**

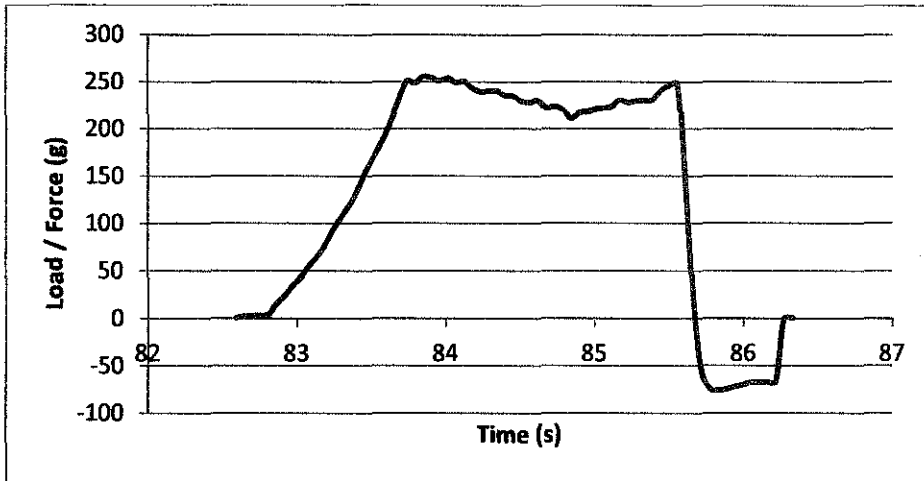


**Figure 12: Octane at 20 wt.% of wax at -4°C**

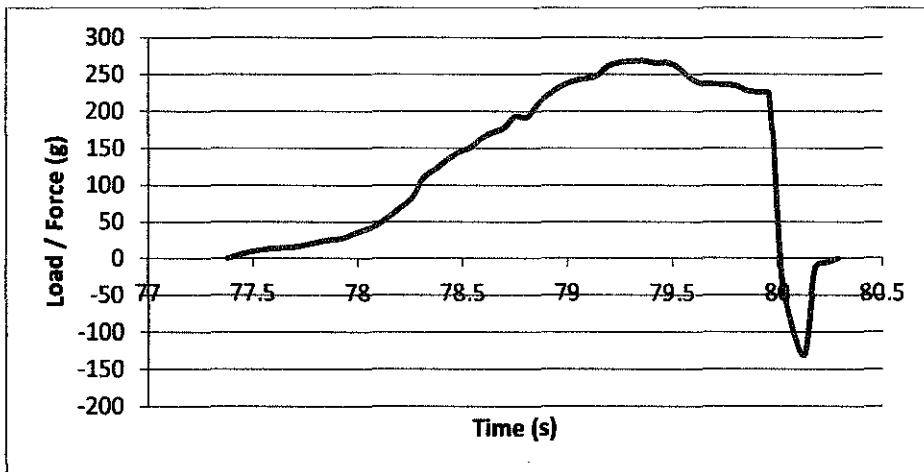


**Figure 13: Octane at 20 wt.% of wax at 0°C**

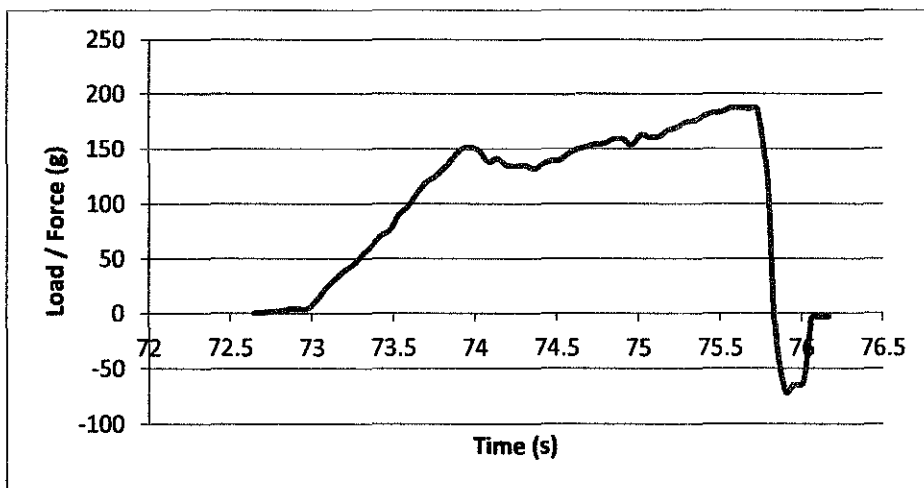


**Figure 14: Octane at 20 wt.% of wax at 10°C**

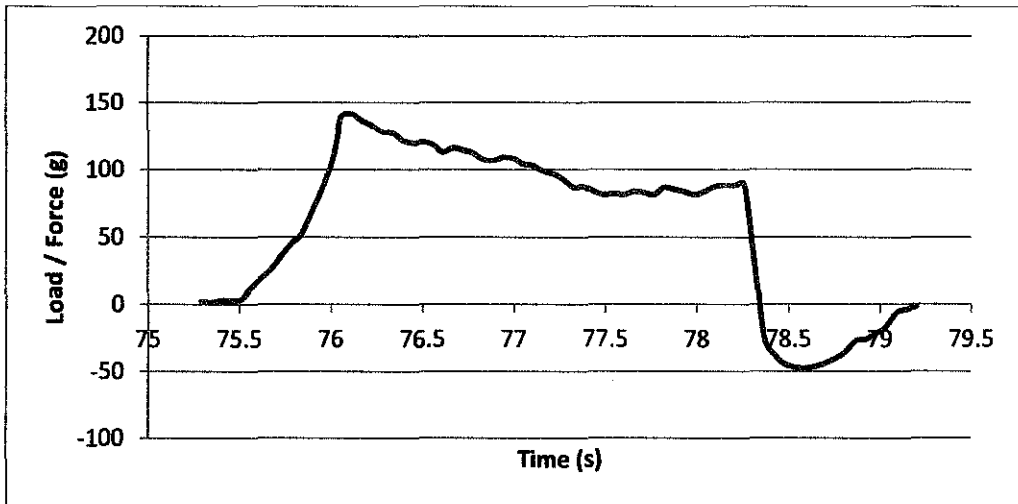


**Figure 14: Octane at 20 wt.% of wax at 25°C**

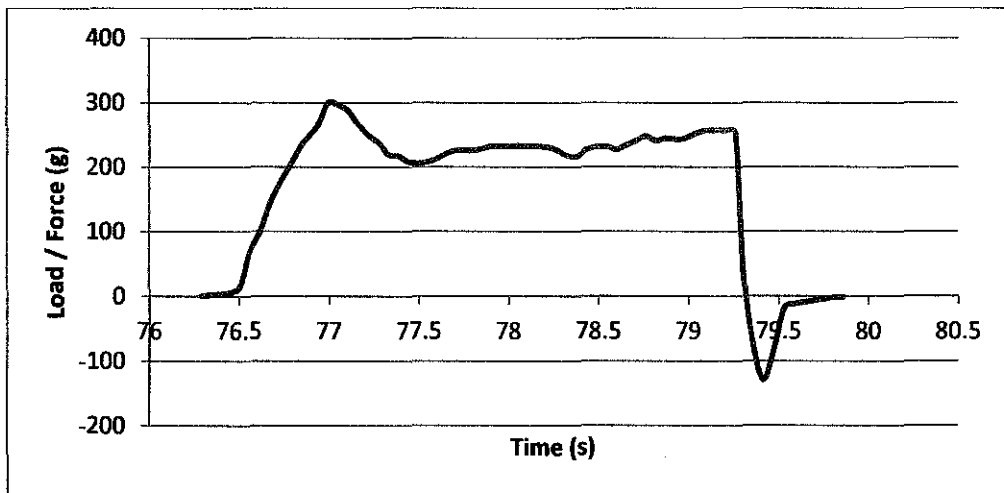


**Figure 15: Octane at 30 wt.% of wax at -4°C**

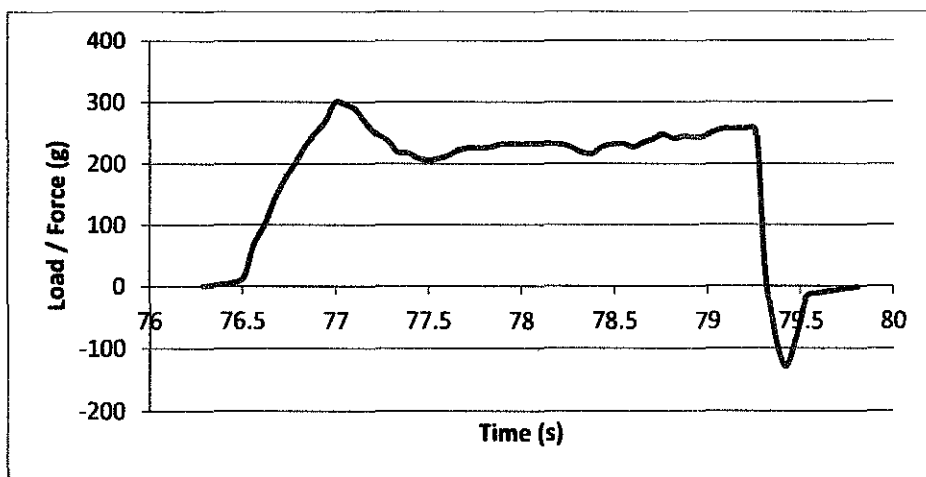


**Figure 15: Octane at 30 wt.% of wax at -4°C**

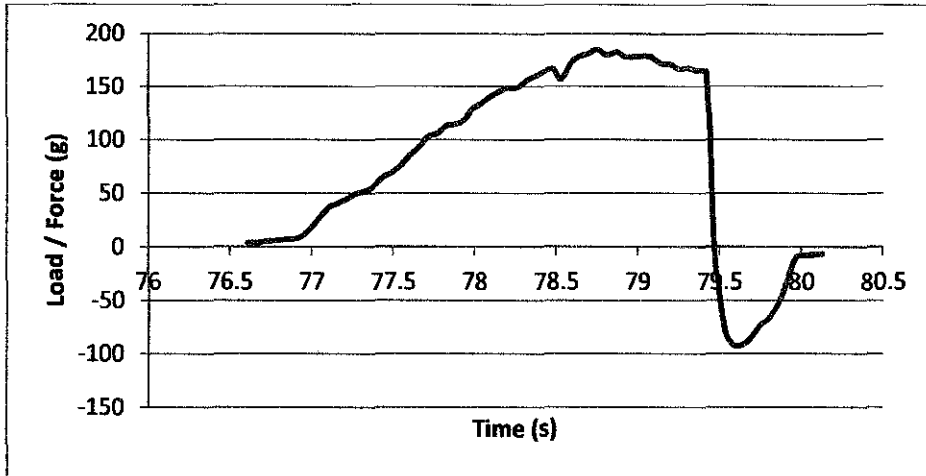


**Figure 16: Octane at 30 wt.% of wax at 0°C**

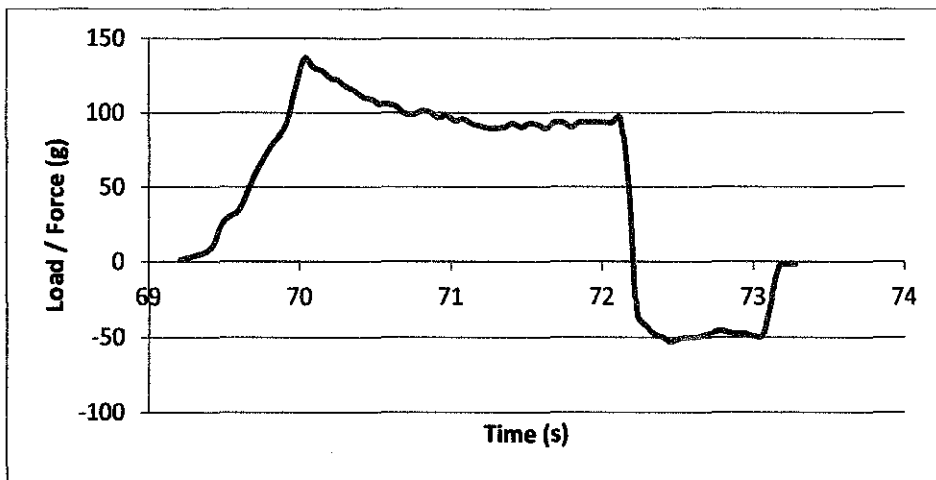


**Figure 17: Octane at 30 wt.% of wax at 10°C**

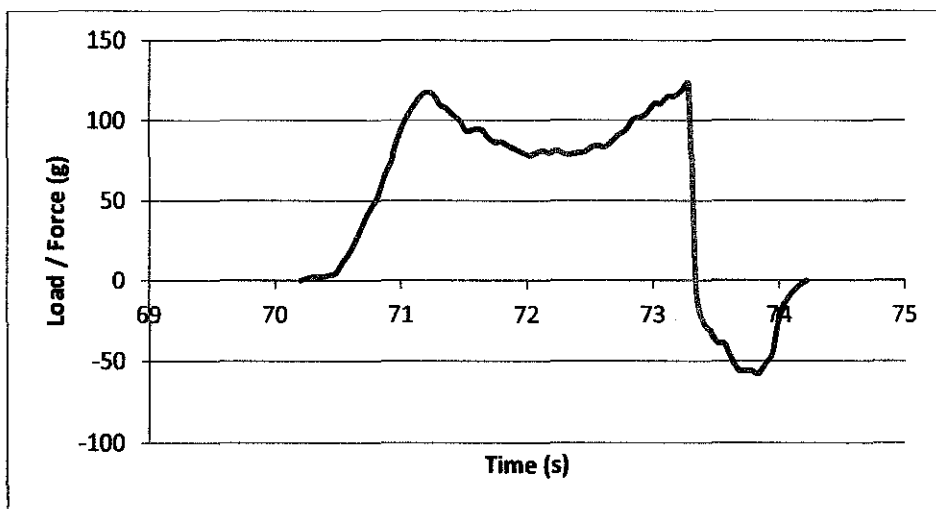


**Figure 18: Hexane at 20 wt.% of wax at -4°C**



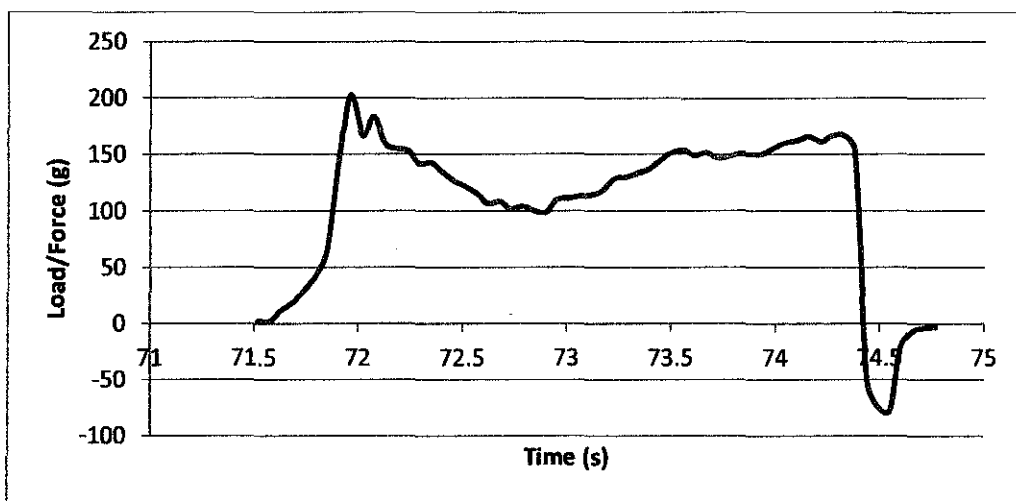


**Figure 18: Hexane at 20 wt.% of wax at -4°C**

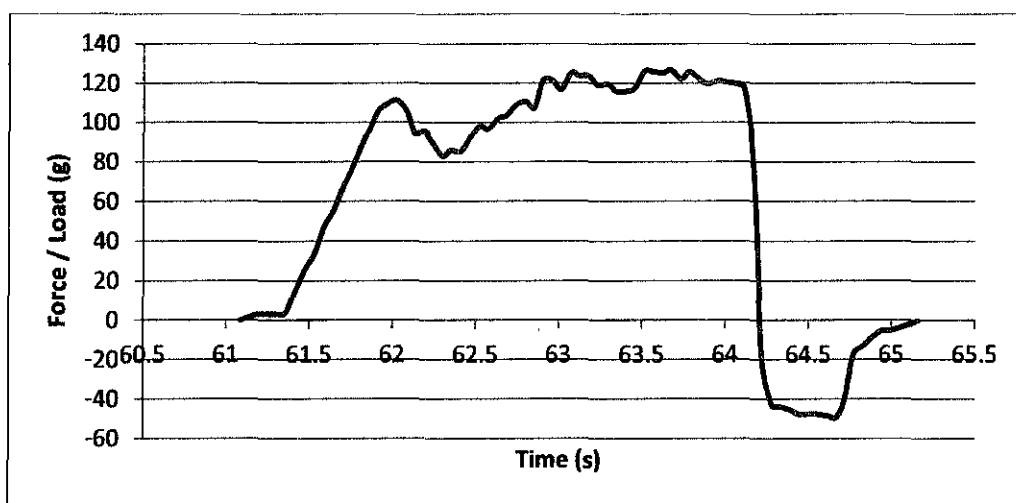


**Figure 19: Hexane at 30 wt.% of wax at 0°C**

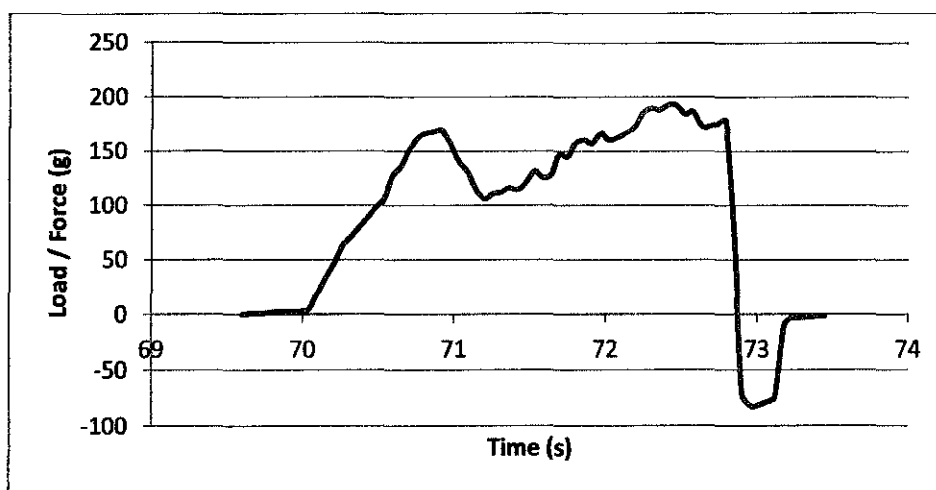


**Figure 20: Hexane at 30 wt.% of wax at 10°C**

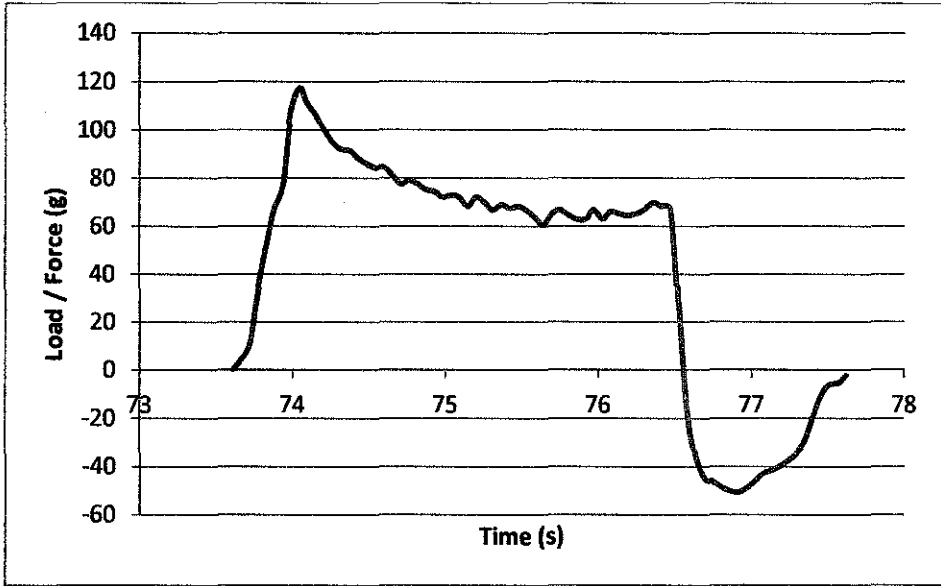


**Figure 21: Hexane at 30 wt.% of wax at 25°C**